

Metal-based catalysts containing a phosphonate moiety – from synthesis to applications in organic chemistry

Mateusz Klarek^a and Magdalena Rapp^{*a}

Faculty of Chemistry, Adam Mickiewicz University
ul. Uniwersytetu Poznańskiego 8, 60-614 Poznań, Poland

Email: magdalena.rapp@amu.edu.pl

In dedication to Professor György Keglevich on the occasion of his 65th anniversary

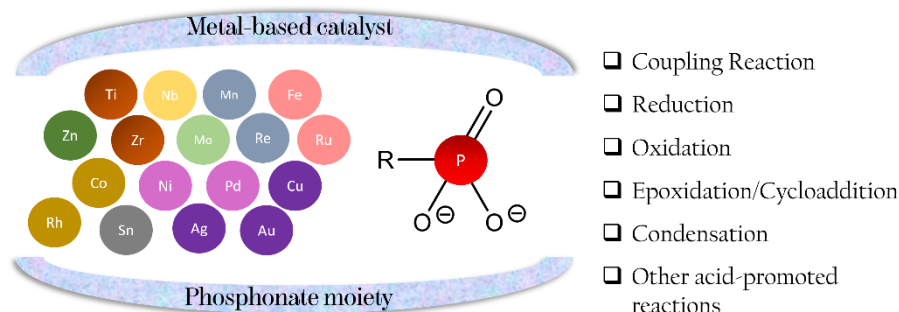
Received 09-30-2022

Accepted 12-11-2022

Published on line 12-21-2022

Abstract

Recently, the development of suitable synthetic methodologies using metal-based catalysts for coupling reactions, oxidation or reduction as well as epoxidation have become topics of great interest. This review article surveys recent achievements in the application of such catalysts as templated porous-metal phosphonates, layered-metal phosphonates, and phosphonate-based metal-organic frameworks (MOFs) in organic syntheses. Additionally, the preparation of various catalysts with defined structure and morphology from organic phosphonate precursors are presented. The versatile properties of phosphonate-containing catalysts offer new and efficient applications in classical as well as modern organic reactions.



Keywords: Catalytic organic synthesis, metal phosphonate, phosphonate catalysts, metal-based catalysts, organic reactions

Table of Contents

1. Introduction
 2. Heterogeneous Catalysts with a Phosphonate Moiety – Applications and Short Characteristics
 - 2.1. Coupling reactions
 - 2.2. Reduction
 - 2.2.1. The reduction of unsaturated C-C bonds
 - 2.2.2. The reduction of C=O bond in aldehydes and ketones
 - 2.2.3. The reduction of nitrocompounds to amines
 - 2.3. Oxidation
 - 2.4. Cycloaddition of CO₂ to epoxide
 - 2.5. Condensations
 - 2.6. Other acid-promoted reactions
 3. Conclusions
- Acknowledgements
- References

1. Introduction

Phosphonates [RPO₃]²⁻ and related [RP(O)₂(OH)]⁻, known derivatives of phosphonic acids RP(O)(OH)₂ due to the presence of a P–C bond, have shown remarkable potential.¹ The capability of coordination and binding properties to suitable metal ions² offers the possibility to create the hybrid metal phosphonates possessing different structures and morphology, as well as physical properties and/or particular chemical reactivity. These materials, distinguished by the presence of extended one-, two-, and three-dimensional structures, are divided into classes, namely layered-metal phosphonates, phosphonate-based MOFs, and templated porous-metal phosphonates.³⁻¹¹ Moreover, the application of organic phosphonates influences the hydrophobic/hydrophilic interactions within materials, frequently enabling the approach of hydrophobic organic molecules to the catalytically-active sites of the metal phosphonate framework. These properties play a significant role in liquid-phase catalytic reactions.

Due to their high chemical and thermal stability as well as high insolubility in many solvents, this class of heterogeneous compounds possesses wide applications, not only in catalytic organic chemistry, but in proton-conduction and energy-storage materials,¹²⁻¹⁶ adsorption and separation,¹⁷⁻¹⁸ biomedical science,¹⁹⁻²¹ and in photocatalytic and electrocatalytic reactions.²²⁻²⁴ The unique combination of organophosphorus precursor(s) and synthetic conditions lead to the desired catalyst to apply in industrial or preparative organic chemistry. Moreover, transition- and some main-group metal elements offer the capability of gain and loss of electrons and/or the corresponding apparent redox ability or Lewis acid-activation properties of the applied catalyst. The additional huge advantage is ease of catalyst recycling, which in turn, affects the economics of the synthesis. For this reason, these compounds are often used in coupling, oxidation, epoxidation, reduction reactions, etc.²⁵⁻

³⁴ The goal of this review is to describe recent advances and achievements, particularly the contributions of the last decade, in efficient syntheses of catalysts based on metal-organic phosphonates scaffolds. Moreover, their use in various types of classical and asymmetric organic transformations will be presented. In this mini-review, the literature is covered from the beginning of January 2010. It is important to supplement this review with some others that have been written on various aspects of metal phosphonates, including designing hybrid

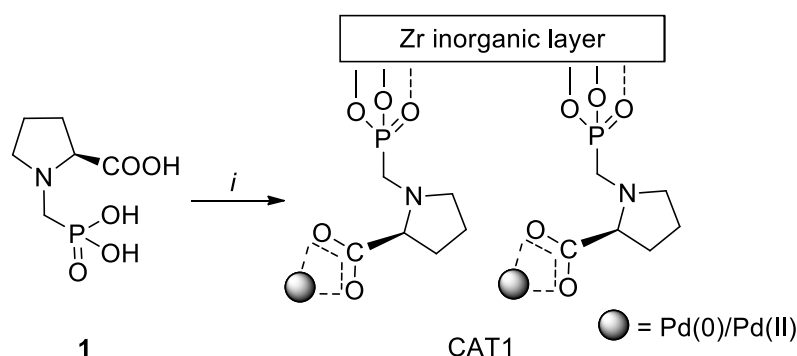
organic-inorganic porous materials and their applications.⁹⁻¹¹ Applications described in these supplemental reviews, including energy conversion and storage, adsorption of heavy metals, membrane materials and photo/electrocatalysis are beyond the scope of the present review.

2. Heterogenous Catalysts with Phosphonate Moiety - Applications and Short Characteristics

2.1. Coupling reactions

One of the most important branches of modern organic chemistry focuses on carbon-carbon bond formation with the application of various types of catalysts.³⁵ Among them, the palladium-assisted coupling reaction is the most widely used.³⁶ Layered materials with a high surface area, and a large amount of exposed active sites, play an important role in the development of new hybrid materials.³⁷ In addition, the possibility of multiple uses of catalysts in subsequent reaction cycles with a very high degree of substrate conversion and their effective recycling, are crucial factors in reducing costs and the amount of waste generated during the reactions.

One of the latest works of Bhattacharyya *et al.* has led to the finding of highly efficient heterogeneous catalysts in the Suzuki-Miyaura cross-coupling reaction.³⁸ The applied catalyst consisted of mesoporous zirconium organocarboxyphosphonate **ZrCP1** which was used as a support matrix for mixed-valent Pd (0) / Pd (II) nano-sized aggregates. The sol-gel system, with the use of surfactants as the pore templates, was employed to obtain the catalyst carrier. The reaction of $\text{ZrOCl}_2 \cdot 8\text{H}_2\text{O}$ with 1-phosphonomethyl-pyrrolidine-2-carboxylic acid **1** was conducted at 130 °C for 3 days with the addition of a cationic surfactant, cetyltrimethylammonium bromide (CTAB). The catalyst support was obtained after treatment with ethanolic HCl for the removal of surfactant. In the next step, **ZrCP1** was impregnated with palladium(II) acetate $[\text{Pd}(\text{OAc})_2]$, which, in combination with the subsequent reduction of absorbed Pd(II), gave CAT1 (Scheme 1). The spectroscopic and structural examinations confirmed the activity of the catalyst beyond the fifth reaction cycle.



Scheme 1. Synthesis of zirconium-based catalyst CAT1. Reaction conditions: *i.* $\text{ZrOCl}_2 \cdot 8\text{H}_2\text{O}$ (1 mmol), CTAB (0.5 mmol), H_2O , next **1** (1 mmol), 130 °C, 3 d, next $\text{Pd}(\text{OAc})_2$ (2.2 mmol), THF, 130 °C, 12h, then NaBH_4 (2.6 mmol), RT, 3h.

Previous works, based on a similar synthetic method, are also known which have proven to be equally effective catalysts in coupling reactions. As the organophosphorus precursors in coupling catalysts, the organophosphonic acids such as mesityl-1,3,5-tris(methylenephosphonic acid **2** and *N,N*-bis(phosphonomethyl)glycine **3** were used (Figure 1).

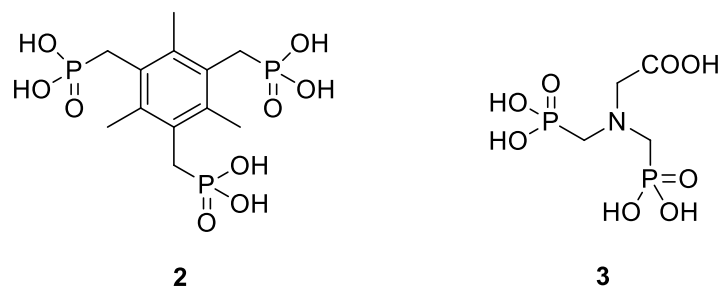


Figure 1. The organophosphorus precursors for the synthesis of CAT2 and CAT3.

The introduction of **2** into layered inorganic solid yielded the organic-inorganic hybrid material. Its applications as a catalyst in Suzuki-Miyaura cross-coupling reactions was reported by Borah *et al.* Thus, the hydrothermal reaction of $\text{ZrOCl}_2 \cdot 8\text{H}_2\text{O}$ with **2**, in the presence of surfactant (CTAB), led to the mesoporous zirconium (IV) phosphonate.³⁹ Next, the final material CAT2 [$\text{Pd}_{0.5}\text{Zr}_3(\text{L})_2$] $x\text{nH}_2\text{O}$, (**Pd@ZrCP2**) was obtained by impregnation of $\text{Pd}(\text{OAc})_2$, followed by reduction with sodium borohydride.

High catalytic efficiency in the reactions of forming new C-C bonds by Suzuki-Miyaura and Heck coupling reactions has been also reported in the case of palladium nanoparticles embedded on zirconium phosphate glycine diphosphonate (ZrPGly) nanosheets CAT3 (**Pd@ZrPGly**).⁴⁰ The layered zirconium phosphate-phosphonate $\text{Zr}_2(\text{PO}_4)[(\text{O}_3\text{PCH}_2)_2\text{NCH}_2\text{COOH}]_2 \cdot x\text{H}_2\text{O}$ (**ZrPGly**) was obtained by the reaction of **3** and zirconium (IV) phosphoric acid. Subsequently, treatment of a colloidal dispersion of **ZrPGly** in *n*-propylamine (PA), with palladium(II) acetate, for 1 or 7 or 15 days gave composites CAT3 with formulas [$\text{Zr}_2(\text{PO}_4)(\text{L})_2\text{Pd} \cdot (\text{PrNH}_2)_2$], $\text{Zr}_2(\text{PO}_4)(\text{L})_2\text{Pd}_{1.5} \cdot (\text{PrNH}_2)_{0.33}$ and $\text{Zr}_2(\text{PO}_4)(\text{L})_2\text{Pd}_{1.92} \cdot (\text{PrNH}_2)_{0.22}$, respectively (Figure 2).⁴¹ The high availability of carboxyl (or COOH), phosphonate (or PO_3H) and amine groups on the surface of the hybrid layers gives these structures polar properties that favor the immobilization and stabilization of palladium particles. Furthermore, it provided confirmation that propylamine in **ZrPGly** dispersion acts as an exfoliating agent, which help to deposit the palladium on the surface of the layer.⁴¹

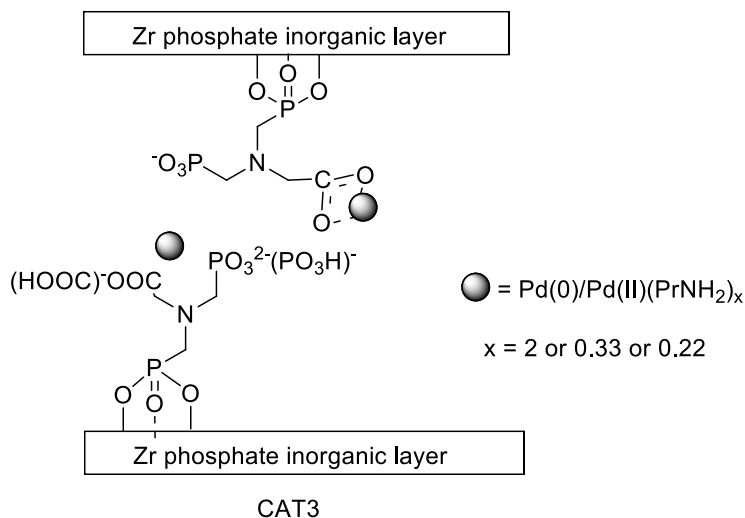
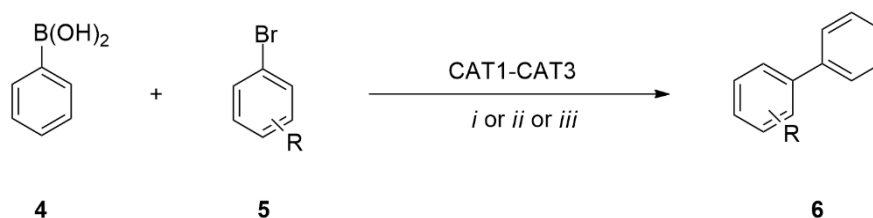


Figure 2. Schematic representation of CAT3.

All of the above described heterogeneous catalysts were tested in a Suzuki-Miyaura cross-coupling reaction of a series of aryl boronic acids **4** with aryl bromides **5** (Table 1).³⁸⁻⁴¹ These catalysts allowed for the

efficient synthesis of various biphenyls **6** substituted with electron-withdrawing or electron donating groups (EWG or EDG), respectively.

Table 1. Suzuki-Miyaura coupling of phenylboronic acid **4** with bromobenzene **5** catalyzed by CAT1 – CAT3

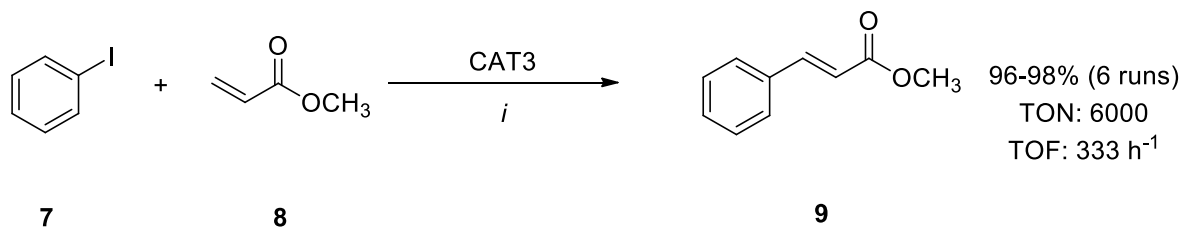


R	CAT1 [%] ^a	CAT2 [%] ^a	CAT3 [%] ^a
<i>p</i> -CN	98	94 ^b	99
<i>p</i> -NO ₂	95	92	98
<i>p</i> -COCH ₃	96	85	99
<i>m</i> -COCH ₃	98	51	-
<i>p</i> -CH ₃	93	22	97
<i>p</i> -OCH ₃	87	29	92
<i>p</i> -CHO	-	-	98 ^c

Reaction conditions: *i.* **4** (0.24 mmol), **5** (0.20 mmol), K₂CO₃ (0.25 mmol), CAT1 (0.22 mol %), EtOH/H₂O (3:1, v:v), 80 °C, 2-10min; *ii.* **4** (0.24 mmol), **5** (0.20 mmol), K₂CO₃ (0.20 mmol), CAT2 (0.15 mol %), EtOH, reflux, 6h; *iii.* **4** (1.0 mmol), **5** (1.2 mmol), K₂CO₃ (1.2 mmol), CAT3 (0.1 mol %), EtOH, 80 °C, 3-24h. ^a yield of **6**, ^b 5 runs: 80-94%, ^c 4 runs: 98%.

It is worth mentioning that coupling reactions catalyzed by CAT3 were performed using azeotropic mixtures (84% CH₃CN in H₂O and 96% EtOH in H₂O) in a flow system, which significantly reduces the amount of organic reaction media. This method allows the catalyst to be recovered, and ensures low metal leaching, as determined by the ICP-OES analysis method. The presented results have confirmed the high catalytic activity of composite materials, giving the possibility of immobilizing palladium nanoparticles and carrying out several reaction cycles.^{40,41}

CAT3 has been proven to be equally effective in Heck coupling reaction of iodobenzene **7** and methyl acrylate **8**, providing complete substrate conversion that led to the formation of a new C-C bond.⁴⁰ The catalyst was used successfully in six reaction cycles with no loss of catalytic activity and afforded **9** in 96 - 98% yields (Scheme 2). It was shown that the leaching of the palladium was at the level of 10 -12 ppm in all of the reaction cycles.



Scheme 2. The Heck reaction of iodobenzene **7** and methyl acrylate **8** catalyzed by CAT3. Reaction conditions: *i.* **7** (6.0 mmol), **8** (7.2 mmol), TEA (7.2 mmol), CAT3 (0.1 mol %), CH₃CN_{aq}, 120 °C, 3h. TOF = turnover number, TON = turnover frequency.

One of the latest works reports three new NHC – Pd(II) complexes (CAT4-CAT6) based on a imidazolium ligand with a pendant phosphonate ester group(s) or phosphonic acid moiety, which have been used as catalysts in C-C bond formation (Figure 3).⁴² Based on the structural analysis, it was determined that the phosphonate ester groups (CAT5 and CAT6) do not participate in the coordination of the palladium atom.

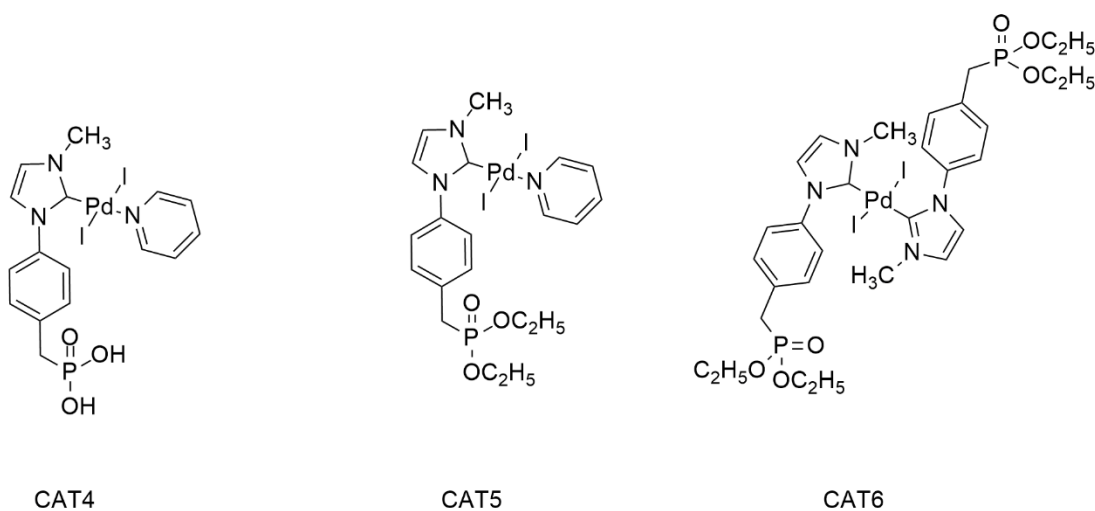
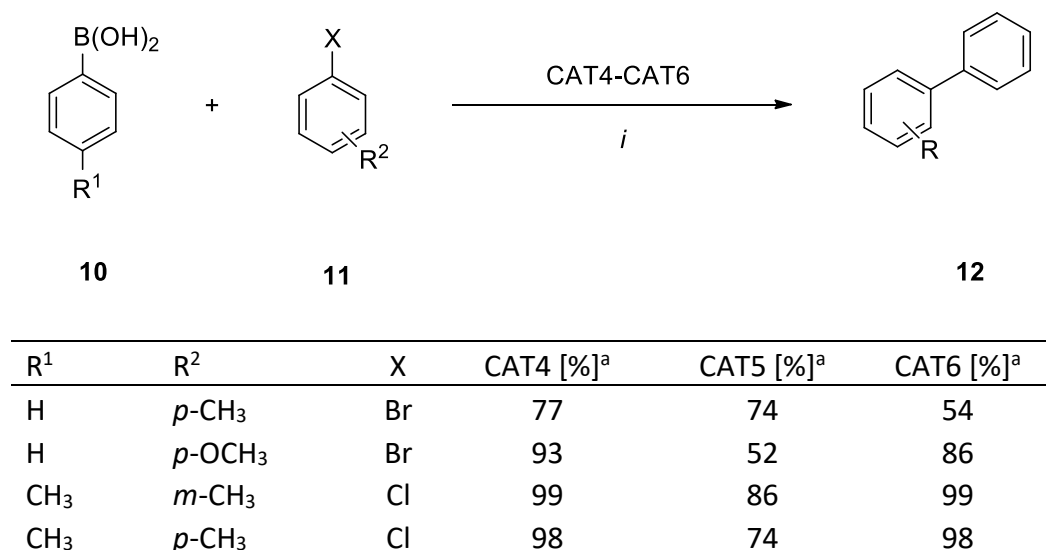


Figure 3. Palladium-based catalyst with phosphonate/phosphonic acid ligands (CAT4 – CAT6).

The obtained catalysts were successfully applied in coupling reactions of aryl boronic acids **10** with substituted aryl chlorides and bromides **11** (Table 2). Moreover, it was confirmed that the catalyst with phosphonic acid moiety (CAT4) showed better catalytic efficiency compared to those containing phosphonate ester groups (CAT5 and CAT6).

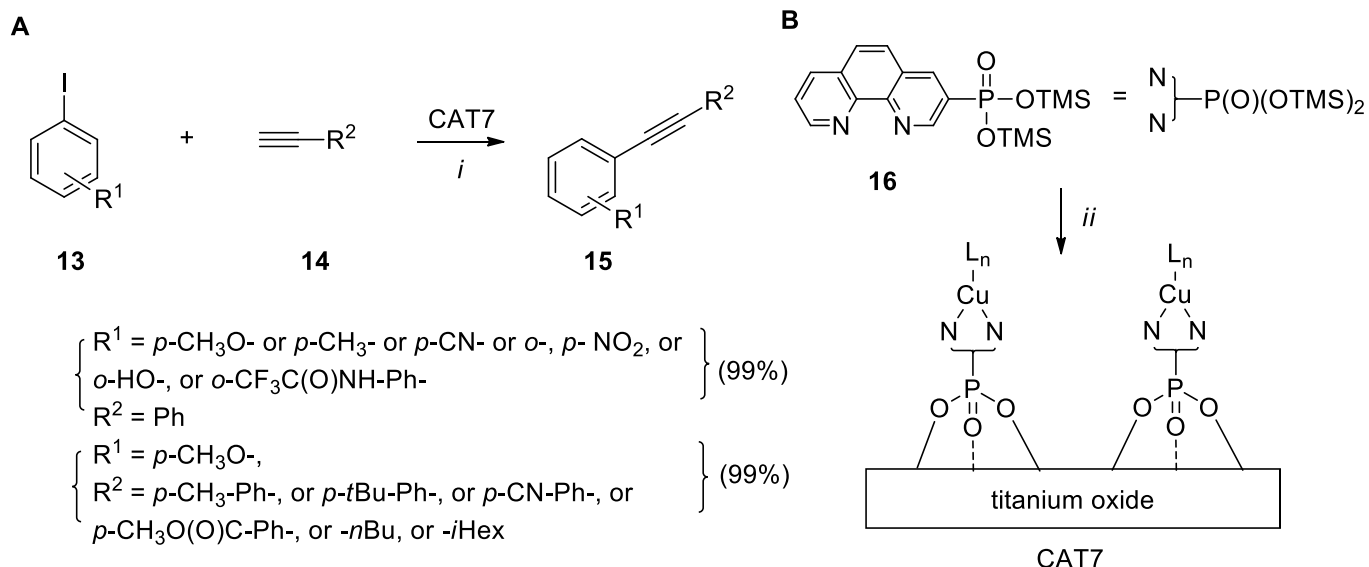
Table 2. Suzuki-Miyaura coupling of phenylboronic acid **10** with bromo- or chlorobenzene **11** catalyzed by CAT4 – CAT6

Reaction conditions: *i.* **10** (0.24 mmol), **11** (0.20 mmol), K₂CO₃ (0.40 mmol), CAT4 – CAT6 (0.5 mol %), *i*PrOH/H₂O (3:1, v:v), 60 °C, 1-6h. ^a yield of **12**.

For comparison, the group of mesoporous TiO₂-supported copper(I) phosphonate-containing catalysts has been also proven to be active in the reactions of forming new C-C bonds in coupling reactions.⁴³ Thus, the Sonogashira-type coupling (Scheme 3 A) can be catalyzed by heterogeneous copper(I) bis 1,10-phenanthroline (phen) complexes anchored by the phosphonate moiety onto the TiO₂ surface (Scheme 3 B). The catalyzed-by-surface-modified CAT7 reactions of aryl iodide **13**, substituted at the *p*- or *o*- positions with the activating [CH₃, *t*-Bu, OH, or NHC(O)(CF₃)] or deactivating (CN, NO₂ or COOCH₃) groups, and an alkyl or aryl acetylene **14** resulted in coupling products **15** in almost quantitative yields (99%). Reactions occurred in applied conditions such as 5% mol catalyst CAT7, PPh₃, Cs₂CO₃, and toluene as a solvent. Additionally, in the case of phenol or aniline derivatives [$R^1 = o$ - OH, or *o*- NHC(O)(CF₃)], the subsequent addition to the triple bond occurs, leading to benzofuran or indole derivatives in excellent yields.

Moreover, the excellent catalytic performance of CAT7 on Huisgen 1,3-dipolar cycloadditions to give substituted 1,2,3-triazoles in yields from 92 - 99% has been presented as well.⁴³

The applied catalyst (CAT7) was obtained from phenanthroline ligands (PPhen) containing the phosphonate moiety [(1,10-phenanthroline-3-yl)phosphonate **16**] grafted onto the mesoporous titanium surface, then complexed with copper(I) ions, e.g., [Cu(MeCN)₄PF₆] (Scheme 3 B). The resulting hybrid material, as well as the integrity of immobilized complexes, were characterized by different physicochemical methods. The CAT7 catalyst was successfully applied in a coupling reaction, leading to complete substrate conversion (99%) in 5 reaction cycles. Alternatively, homoleptic and heteroleptic copper(I) complexes of variously-substituted phenanthroline-bearing phosphonate groups were prepared from bis(trimethylsiloxy)phosphoryl derivatives of phenanthroline **16** (PPhen) and, next, embedded into TiO₂ or grafted onto the TiO₂ surface.⁴³



Scheme 3. A. The Sonogashira coupling reaction between aryl iodide **13** and R^2 -acetylene derivatives **14**, catalyzed by CAT7; B. Synthesis of copper complexes on titanium oxide (CAT7). Reaction conditions: *i.* **13** (0.5 mmol), **14** (0.75 mmol), CAT7 (5 mol %), PPh_3 (10 mol %), Cs_2CO_3 (1 mmol), PhCH_3 , reflux, 16h; *ii.* **16**, TiO_2 , next $\text{Cu}(\text{CH}_3\text{CN})_4\text{PF}_6$.

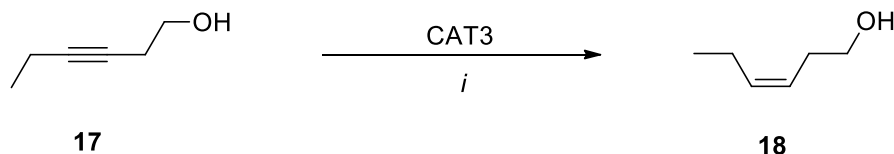
This part involving the coupling reaction has been reflecting the growth of application of metal-organic phosphonate-based catalysts or organic-inorganic hybrid-phosphonate materials. On the other hand, this group of materials is widely present and useful in organic syntheses involving reduction or oxidation reactions.

2.2. Reduction

It is often necessary to reduce, selectively, one group in a molecule without affecting another reducible group. The most common broad-spectrum reducing agents are metal hydrides and hydrogen with a catalyst. Many different hydrogenation catalysts have been investigated in order to find optimal conditions under which a given group will be reduced chemoselectively. Some catalysts, especially containing Pd, Rh, Ru or Ni, are particularly selective towards the reduction of certain classes of compounds.^{44,45} Below, various reducing catalysts are listed, representing their reactivity of various functional group.

The reactions in this section are grouped into classifications based on bond changes: reduction of triple to double C=C bond, or reduction of a carbonyl C=O group or transformation of nitro compounds into amines. In some cases, the catalytic reduction, followed by intramolecular transesterification, was described.

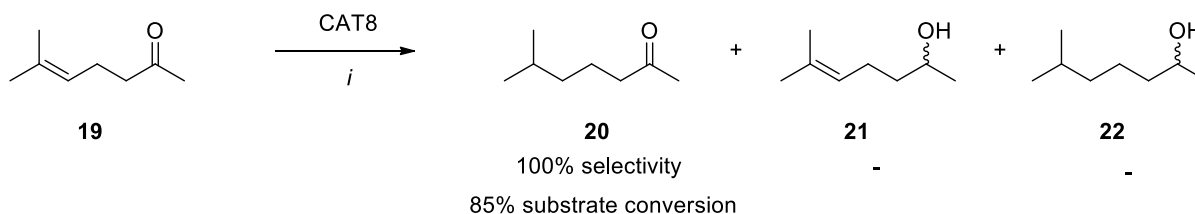
2.2.1. The reduction of unsaturated C-C bonds. One of the most applied reactions is the stereoselective reduction of triple bonds using catalytic palladium-based hydrogenation. Among various heterogeneous palladium-containing catalysts, the zirconium phosphate-phosphonate nanohybrid material has also been used.⁴⁶ The nanosheet-form catalysts containing different propylamine contents were prepared as described for CAT3 by changing the initial amount of propylamine (PA) as an exfoliating agent (20, 40, 60 and 80% of the ion exchange capacity). The reduction of alkyne **17** has been shown to proceed selectively to give *Z*-alkene **18** and, moreover, the leaching of palladium in the solution was negligible (Table 3).

Table 3. Reduction of 3-hexyn-1-ol **17** catalyzed by CAT3 containing different amounts of propylamine (PA)

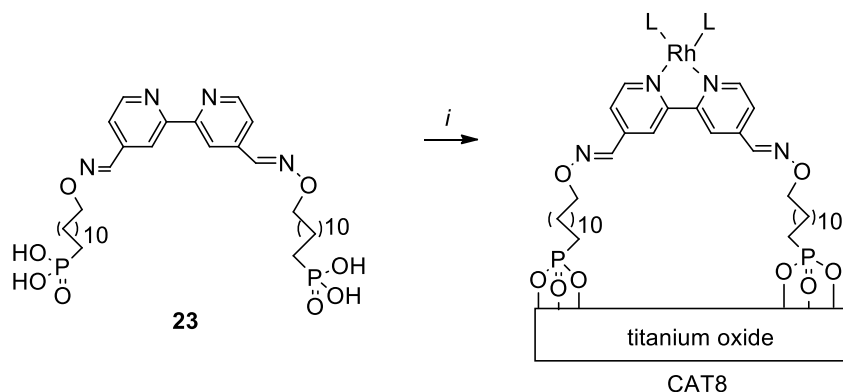
Catalyst	Pd% [w/w]	Conversion [%]	TOF [h ⁻¹]	Z-Sel. [%] ^a
CAT3-20-PA	19.8	99.9	480	91.2
CAT3-40-PA	19.4	99.0	297	95.9
CAT3-60-PA	21.7	99.2	397	96.5
CAT3-80-PA	19.4	99.9	150	89.8

Reaction conditions: *i.* **17** (0.2 M, MeOH), H₂, 0.1 MPa, **17**/CAT3 ratio (mol/mol): 400. ^a Z-selectivity (**18**/sum of the products).

The chemoselective catalytic efficiency in the hydrogenation reactions has also been reported using heterogeneous rhodium complexes of phosphonate-containing 2,2'-bipyridine (bipy) ligands on titanium oxide.⁴⁷ The obtained catalysts have been used for the reduction of 6-methyl-5-hepten-2-one **19** under hydrogen pressure (4 MPa) to give **20** as the main product (Scheme 4). It was found that the application of CAT8 led to 85% substrate conversion, and 100% selectivity for hydrogenolysis of C=C bonds to get **20**. Analogous reductions of **19** using catalysts containing other 2,2'-bipyridine ligands gave substrate conversion from 15 - 99% and distribution of products **20-22** from 70 - 100%, respectively.

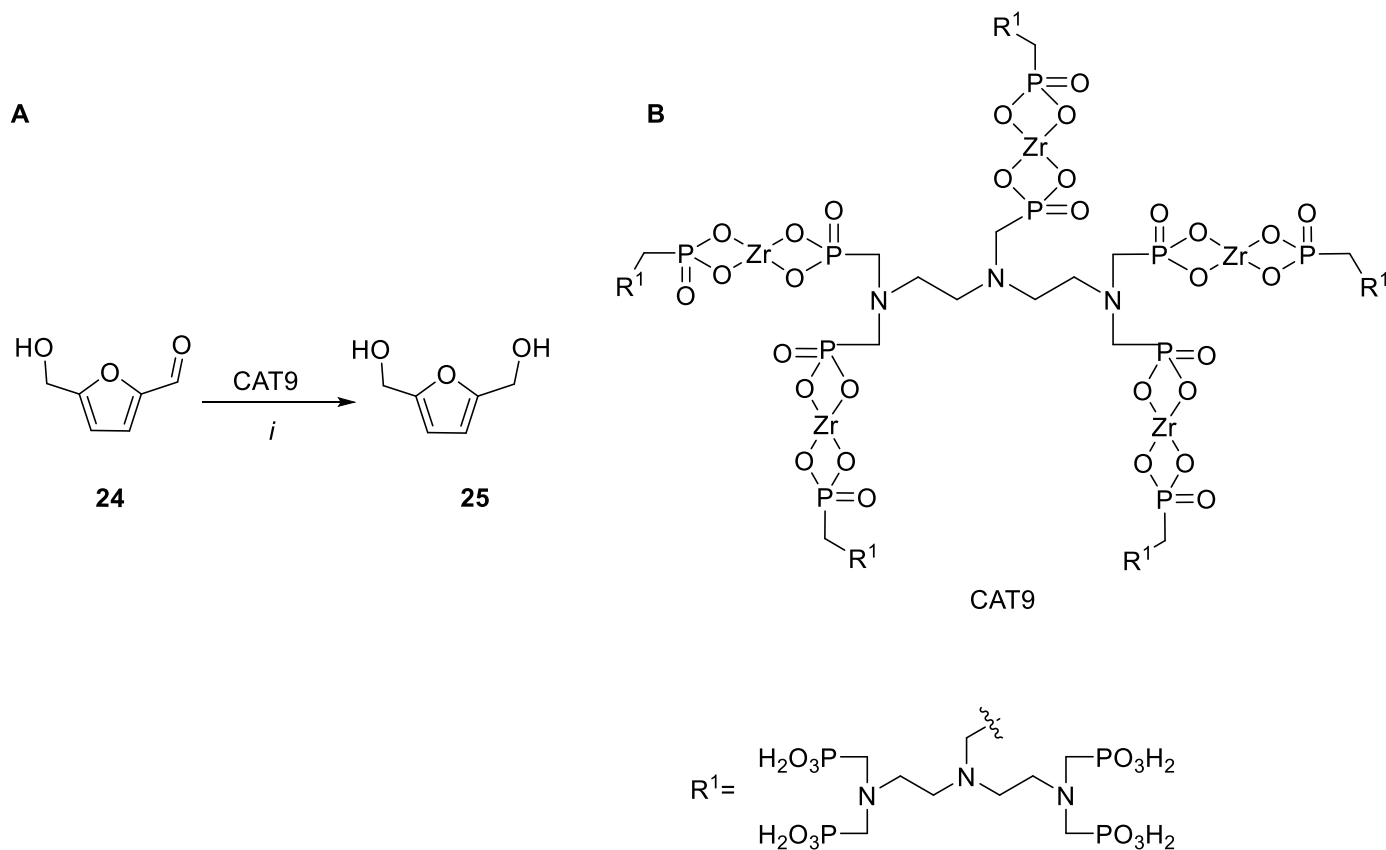
**Scheme 4.** Reduction of 6-methyl-5-hepten-2-one **19** catalyzed by CAT8. Reaction conditions: CAT8/**19** (molar ratio 1%), H₂, NaOH/MeOH, 4 MPa, 30 °C, 4h.

The most efficient CAT8 was prepared by immobilization of a RhL₂ complex, containing bipy ligands with covalently-bonded dodecyl linkers ending with phosphonate groups (e.g., **23**), on titanium oxide particles (Scheme 5). Due to diverse phosphonate-bipy arrangements depending on the ligands substitution and the numbers of tethers in the RhL₂ species, influencing both microstructures and the location at the solid surface, different catalytic efficiencies have been reported.



Scheme 5. Synthesis of rhodium complex RhL_2 on titanium oxide CAT8. Reaction conditions: **23**, $[Rh(COD)(Cl)_2]^a$ (0.0395 mmol), $AgBF_4$ (0.079 mmol), MeOH, RT, 1h, next 2,2'-bipyridine (0.16 mmol), 5 min, NaOH (1M), then $Ti(OiPr)_4$, 2d. ^aCOD – 1,5-cyclooctadiene.

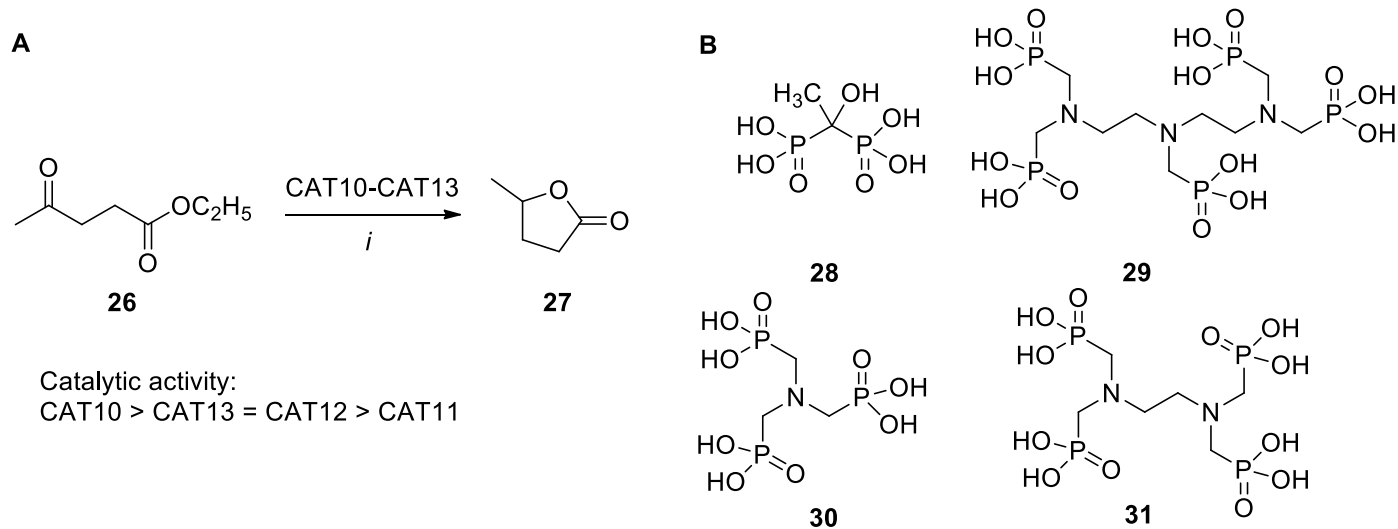
2.2.2. The reduction of C=O bond in aldehydes and ketones. There are various possibilities for reducing the carbonyl group of aldehydes and ketones to alcohols. The most common methods consist of the use of nucleophilic or electrophilic hydrides, hydrogen on platinum and ruthenium catalysts or metal in water, etc.⁴⁸ Less popular reductions based on Pt or Ru catalysts suffered from lower chemoselectivity resulting from additional C=C or C=N reductions in the cases of unsaturated- or imine-containing ketones or aldehydes. For comparison, a high reaction efficiency (nearly 97%) under relatively mild conditions was reported for the Meerwein-Ponndorf-Verley (MPV) reduction of 5-hydroxymethylfurfural (HMF) **24** to 2,5-dihydroxymethylfuran (DHMF) **25**, which can be useful as a polymer precursor derived from renewable biomass resources.⁴⁹ Thus, to obtain **25**, zirconium phosphonate catalyst CAT9 (**Zr-DTMP**) has been used (Scheme 6 A).⁵⁰ A mesoporous zirconium organic-inorganic material (Scheme 6 B) was obtained by easily combining metal ions with suitable ligands. For this purpose, the solutions of diethylene triaminepenta(methylene phosphonic acid) (DTMP) and zirconium tetrachloride ($ZrCl_4$) were combined and then TEA was added. The obtained catalyst was successively used in five runs.



Scheme 6. A. Reduction of 5-hydroxymethylfurfural **24** catalyzed by CAT9; B. The structure of CAT9. Reaction conditions: *i.* **24** (0.5 g), CAT9 (0.3 g), *sec*BuOH (24.5 g), 140 °C, 3h.

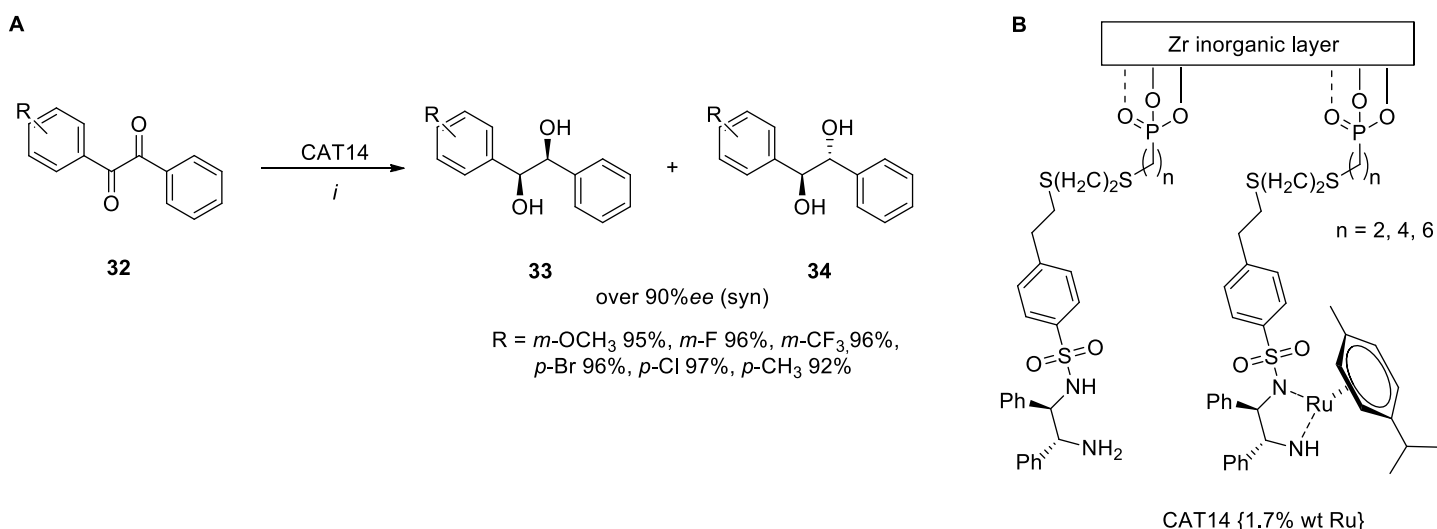
Interestingly, it's the first example of the application of CAT9 for the synthesis of **25**. Furthermore, this catalytic system can also be used in selective reduction of levulinic acid (LA), ethyl levulinate (EL) and many others.⁵⁰

An additional application of zirconium phosphonates in reduction reactions has been shown by Wang *et al.*⁵¹ The authors showed that hybrid zirconium phosphonate materials CAT10 (**ZrHEDP**), CAT11 (**ZrDTPMP**), CAT12 (**ZrATMP**), CAT13 (**ZrEDTMP**) are efficient catalysts for the catalytic transfer hydrogenation of ethyl levulinate (EL) **26** to γ -valerolactone **27** without external delivery of hydrogen (Scheme 7 A). Hybrid materials were obtained through the reactions of organophosphonic acids such as 1-hydroxyethylidene-1,1-diphosphonic acid (HEDP) **28**, diethylene triaminepenta(methylene phosphonic acid) (DTPMPA) **29**, ATMP **30**, and ethylenediamine tetra(methylene phosphonic acid) (EDTMP) **31**, in forms of sodium salts (Scheme 7 B), with ZrOCl₂ in water by the co-precipitation method. The catalysts were reused and demonstrated activity in no fewer than five reaction cycles.



Scheme 7. A. Catalytic transfer hydrogenation of ethyl levulinate **26** catalyzed by CAT10 – CAT13; B. Organophosphorus precursors **28** – **31** used for the synthesis of CAT10 – CAT13. Reaction conditions: *i.* **26** (1 mmol), CAT10 – CAT13 (200 mg), *i*-PrOH, 160 °C, 9-12h.

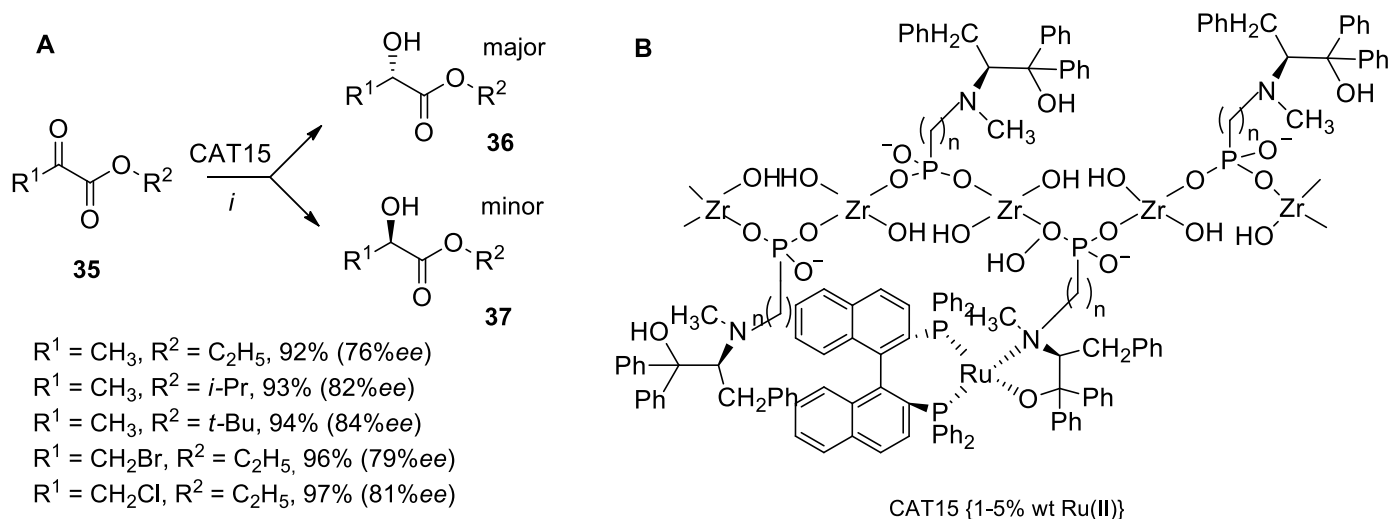
Another widely studied reaction involves the reduction of the C=O bond with the use of zirconium-phosphonate-supported ruthenium catalysts. In particular, Du *et al.* have applied a chiral Ru catalyst in asymmetric hydrogenation of unsymmetrical benzyls **32** to hydrobenzoin **33**, and **34** (Scheme 8 A).⁵² This work is based on the translation of heterogeneous catalysis of a zirconium-phosphonate-supported ruthenium catalyst, in a homogeneous system, by covalent attachment of (*R,R*)-1,2-diphenylethylenediamine [(*R,R*)-DPEN] into zirconium phosphonate followed by immobilization of [RuCl₂(*p*-cymene)]₂. The obtained catalyst (CAT14, Scheme 8 B) ensures excellent activity and high substrate **32** conversion.



Scheme 8. A. Hydrogenation of unsymmetrical benzyls **32** catalyzed by CAT14; B. The structure of CAT14. Reaction conditions: *i.* **32** (0.084 mmol), CAT14 (1.7 wt%, 6.7×10^{-4} mmol), HCOOH/TEA (1:2, v:v), 50 °C, 40h.

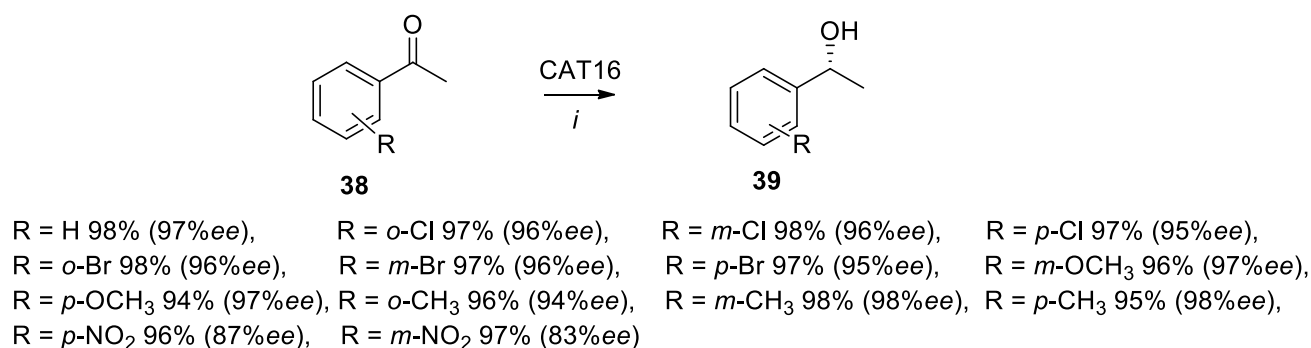
Moreover, the zirconium-phosphonate-supported ruthenium catalysts were tested in reduction reactions, especially in asymmetric hydrogenations.⁵³ The supported ruthenium catalyst was obtained by the

reaction of zirconium phosphonate with Ru(*p*-cymene)(*S*-BINAP)Cl₂ (BINAP = 2,2'-bis(diphenylphosphino)-1,1'-binaphthyl) in an inert-gas atmosphere (CAT15, Scheme 9 B). The catalyst activity was measured in the asymmetric hydrogenation of diversely substituted α -ketoesters **35** (Scheme 9 A) to give hydroxyesters with yields of up to 97%, and with high enantioselectivities up to 84% *ee*. The values obtained were greater in relation to the parent Ru(*p*-cymene)(*S*-BINAP)Cl₂ than with what could be strongly correlated to the effect of confinement of the remaining mesopores in the zirconium phosphonate.



Scheme 9. A. Asymmetric hydrogenation of α -ketoesters **35** catalyzed by CAT15; B. The structure of CAT15. Reaction conditions: *i.* **35**/CAT15 ratio = 250, H₂, 4.05 MPa, 80 °C, 1h.

In comparison to zirconium-phosphonate framework as a catalyst, Xu *et al.* reported highly efficient, chemo- and enantio-selective polystyrene-copolymer-supported Ru catalysts in the asymmetric reduction of carbonyl compounds in water.⁵⁴ The reactions performed in water as a solvent are an important trend in green chemistry and have attracted a lot of attention. In this case, the excellent catalytic properties were proven in the transfer hydrogenation of aromatic ketones **38**, having either electron-donating or withdrawing substituents, in water, as an environmentally friendly, protic, polar solvent (Scheme 10).



Scheme 10. Asymmetric transfer hydrogenation of acetophenone **38** catalyzed by CAT16. Reaction conditions: *i.* **38** (0.86 mmol), CAT16 (1.5 wt% Ru), H₂O, HCOOH/TEA (1:3, v:v), 50 °C, 6h.

The resulting alcohols [(*R*)-configuration] were obtained in high yields (94 - 98%) and enantioselectivities (94 – 98% *ee* except for the *m*-NO₂ derivatives) depending on the linker between polystyrene and the ligands (with the most efficient catalyst being CAT16, containing a sulfonamide moiety bonded directly to the phenyl ring). Surprisingly, reduction of the *o*-anisole derivatives (R = *o*-OCH₃) gave (*S*)-alcohol with 96% yield and 94% *ee*. The applied catalysts were obtained from phosphonates possessing co-polystyrenes bound to the ligands (1*R*,2*R*)-(+)-*N*-1-toluenesulfonyl-1,2-diphenylethylene-1,2-diamine *via* different nitrogen-containing linkers (Figure 4).

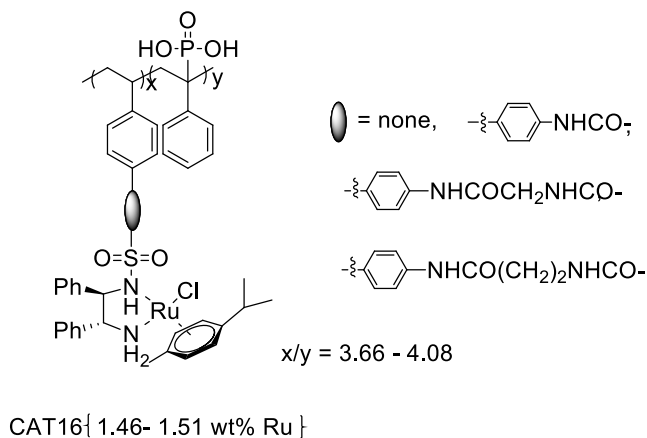
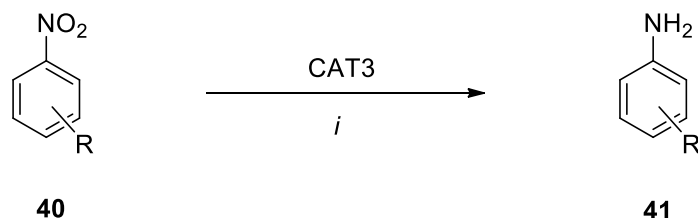


Figure 4. The structure of polystyrene Ru catalysts CAT16.

The synthesis involved radical copolymerization of 1-phosphonate styrene with styrenes bearing a linker connected to chiral 1,2-diamine [in the presence of benzoyl peroxide (BPO), THF, 80 °C, 24h], followed by immobilization of [RuCl₂(*p*-cymene)]₂. The obtained polystyrene copolymers containing Ru particles trapped in nanopores play the role of diffusional channels allowing substrates to access the catalytic sites. Introduction of phosphonate to polymer as supports increased polarity of the polystyrene-based catalyst and solubility in alcohol. Moreover, it was suggested that phosphonate acts as a surfactant, indicated by the good dispersion upon adding TEA in the catalytic reaction. This catalyst can be recycled by centrifugal separation and reused in five consecutive runs.

2.2.3. The reduction of nitrocompounds to amines. Both aliphatic and aromatic compounds containing a nitro group can be reduced to amines or anilines. The most common methods are catalytic hydrogenation or application of some metal, e.g., Zn, Sn or Fe, and an acid.

Among various heterogeneous palladium-containing catalysts, the zirconium phosphate–phosphonate nanosheet material – CAT3 (described in the coupling reactions section)⁴² caused the reduction of aromatic nitro compounds **40** to give aniline derivatives **41** (Table 4). The results showed that the amount of Pd loading on the CAT3 catalyst does not greatly affect the selectivity, and the catalytic efficiency is closely related to the nature of the substituent on the aromatic ring. The presence of a halogen atom in the *meta* position significantly accelerated the kinetics of the reaction (TOF of 683 h⁻¹ for *m*-chloronitrobenzene), while the unsubstituted nitrobenzene was the least reactive (TOF of 50 h⁻¹ for nitrobenzene). Complete chemoselectivity (100%) was achieved for the *meta*-substituted fluorine derivatives, while, in the case of chloro and aldehyde derivatives, the chemoselectivity decreased to 84%.

Table 4. Catalytic reduction of nitrobenzene derivatives **40** catalyzed by CAT3

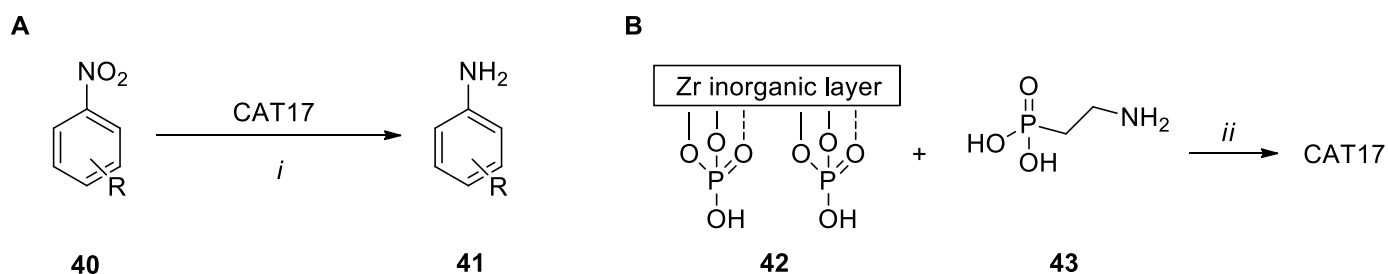
72%-99% substrate conversion

84%-100% chemoselectivity

R	Cycle	40 /CAT3 ratio	Time [min]	Conversion of 40 [%]	TOF [h ⁻¹]
H	1	100	120	99.9	50
<i>m</i> -Cl	1	300	20	75.3	683
<i>m</i> -F	1	200	60	99.9	200
<i>m</i> -F	2	200	60	99.9	200
<i>m</i> -F	3	200	60	98.5	197
<i>p</i> -Br	1	200	60	72.4	145
<i>p</i> -CHO	1	200	105	99.3	137

Reaction conditions: *i.* **40** (0.2 M, MeOH), H₂, 0.5 MPa, RT.

Nitroarene reductions can also be catalyzed by Au@Zirconium-Phosphonate Nanoparticles. In 2019, Ferlin *et al.* presented an inorgano-organic layered material that can be used as an effective catalytic system for the chemoselective, mild, and switchable, reduction of nitroarenes.⁵⁵ The gold-based catalyst CAT17 [Au@ZrP(AEP)] was tested in the chemoselective reduction of a series of nitroarenes **40** to substituted aminoarenes **41** in EtOH (96%) or EtOH_{abs} (Scheme 11 A). This process is highly efficient and economical because the catalyst can be recycled and reused in the flow-system reaction.



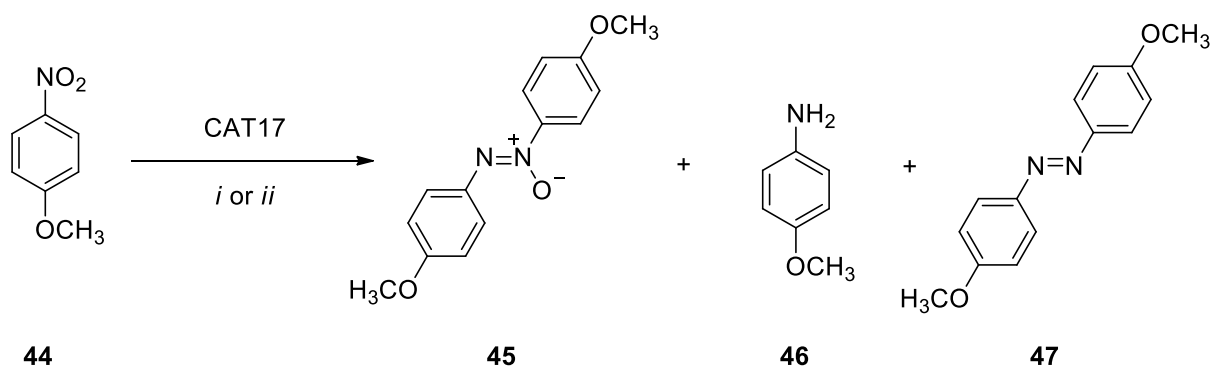
R = H, *p*-OMe, *p*-Cl, *p*-Br, *p*-Me, *m*-Me, *o*-Me, *m*-CH₂=CH₂, *m*-COMe, *p*-COMe

Scheme 11. A. Reduction of nitrobenzene derivatives **40** catalyzed by CAT17; B. The synthesis of CAT17. Reaction conditions: *i.* **40** (0.1 mmol), CAT17 (1 mol %), NaBH₄ (6eq.), EtOH_{abs}, 30 °C, 1-6h; *ii.* **42** in PrOH (1g of **42**/14 mL PrOH), **43** (**43**/Zr molar ratio: 1 or 2 or 3), 80 °C, 3 d.

It was proven that the zirconium phosphate aminoethyl phosphonate ZrP(AEP) is suitable for immobilizing gold nanoparticles. The starting material for the synthesis of ZrP(AEP) was prepared using

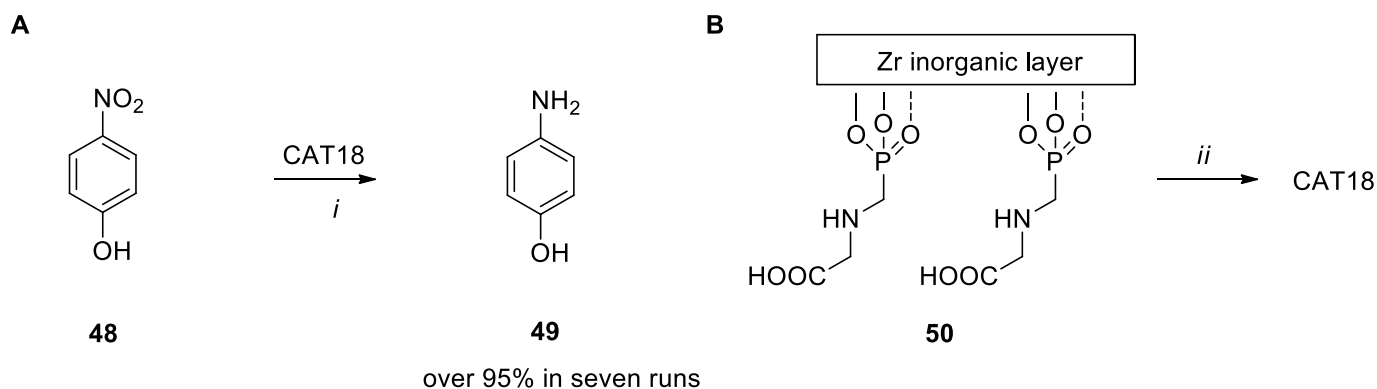
zirconium phosphate **ZrP** gel in alcohol (PrOH) based on a Pica *et al.* method.⁵⁶ Thus, in the first step, a solution of zirconyl phosphate in anhydrous alcohol was prepared, and then concentrated phosphoric acid was added to obtain the $\text{H}_3\text{PO}_4/\text{Zr}$ molar ratio (R) equal 2, 4, or 6, respectively, and $[\text{H}_3\text{PO}_4] < 2$ M. The introduction of amino groups was possible by means of an anion exchange reaction of the phosphates moiety with the incoming aminoethylphosphonic acid H_2AEP **43** (Scheme 11 B). Finally, the gold nanoparticles were supported on **ZrP(AEP)0.7**. For this purpose, a solution containing AuCl_4^- ions was added to a **ZrP(AEP)** suspension and then reduced with sodium borohydride.

It was also noticed that the used solvent had an effect on the chemoselectivity of the reduction of **44**. In the case of ethanol (96%), the main product was the azoxy derivative **45**, while use of absolute ethanol led to the aniline derivative **46**. Moreover, traces of compound **47** were observed (Scheme 12).



Scheme 12. Reduction of 1-methoxy-4-nitrobenzene **44** catalyzed by CAT17. Reaction conditions: **44** (0.1 mmol), CAT17 (1 mol %), NaBH_4 (6eq.), 30 °C, 3h; *i*. EtOH (96%): 5 runs (87 – 98% conversion of **44**), products ratio: **45:46:47** aver. 97:0:3; *ii*. EtOH_{abs}: 5 runs (>99% conversion of **44**), products ratio: **45:46:47** 0:100:0.

In the last few years, a new type of composite of silver nanoparticles (**AgNPs**) supported by zirconium glyphosate (**ZrGP**) has been proposed.⁵⁷ The tests conducted confirmed the high catalytic activity of the designed composite in the reduction of *p*-nitrophenol (*p*-NP) **48** to *p*-aminophenol **49** using freshly prepared NaBH_4 (Scheme 13 A).



Scheme 13. A. Reduction of *p*-NP **48** catalyzed by CAT18. B. The synthesis of CAT18. Reaction conditions: *i*. **48** (H_2O , 0.1 mmol/L), NaBH_4 (H_2O , 0.5 M), CAT18 (10 mg), 25 °C, 10min; *ii*. **50** (0.44 g), AgNO_3 (0.05 M), H_2O , 80 °C, 6h, then sodium citrate (100 mL, 0.5 M), 98 °C, N_2 .

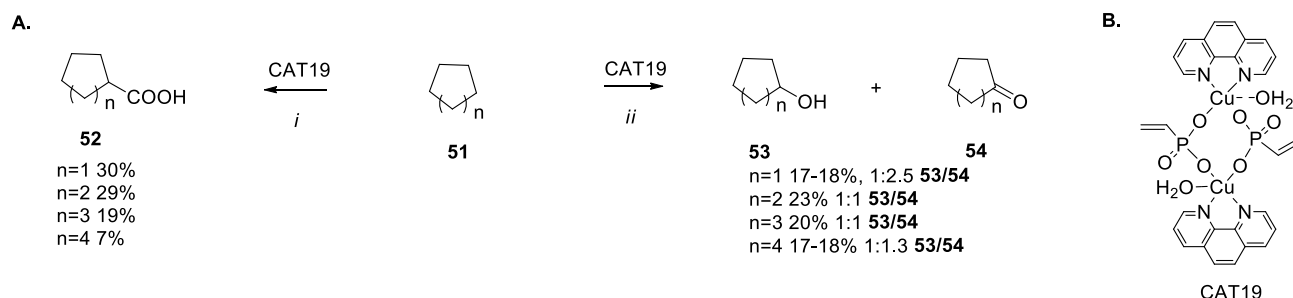
The catalyst could be used 7 times without a clear decrease in conversion of **48**. The reaction rate was monitored by UV-Vis absorption; a decreasing band intensity at 400 nm and gradual discoloration of the solution were observed. **ZrGP** nanosheets **50** were obtained *via* reaction with $\text{ZrOCl}_2 \times 8\text{H}_2\text{O}$ and 40% hydrofluoric acid; the resulting mixture was added to glyphosate in deionized water. A multifunctional nanocomposite CAT18 (**Ag/ZrGP**) was prepared *in situ* by mixing AgNO_3 and **50** (Scheme 13 B). Similar conversion of 4-nitrophenol **48** to 4-aminophenol **49** using NaBH_4 and mesoporous nickel phosphate/phosphonate hybrid microspheres, prepared by phosphate-mediated self-assembly methodology was also reported.⁵⁸

Many reduction reactions with participation of a phosphonate-containing catalyst were considered in the previous chapter, however, some oxidation of organic compounds can be accomplished by application of phosphonate precursors as well.

2.3. Oxidation

The reactions in this section are classified into groups depending on the type of bond change involved. These groups are reactions involving the replacement of hydrogen by oxygen (oxidation of hydroxyl group, thioether to sulfoxide, methylene moiety to carbonyl group or aldehydes to carboxylic acids). We included in this category as well, reactions in which oxygen is added to the substrate (epoxidation) and transformations of ketones or aldehydes to carboxylic esters in the Baeyer-Viliger rearrangement.

The oxidation of a methylene group in cycloalkanes **51** has been made using a di-copper (II) complex containing vinylphosphonic acid (VPA) and 1,10-phenanthroline (phen) (Scheme 14). Thus, the CAT19 $[\text{Cu}_2(\mu\text{-VPA}_2)(\text{phen})_2(\text{H}_2\text{O})_2]$ complex has been examined as efficient catalysts for the mild oxidation or hydrocarboxylation of cycloalkanes **51**, leading to carboxylic acid **52** or a mixture of primary alcohols **53** and ketones **54** (Scheme 14 A).⁵⁹

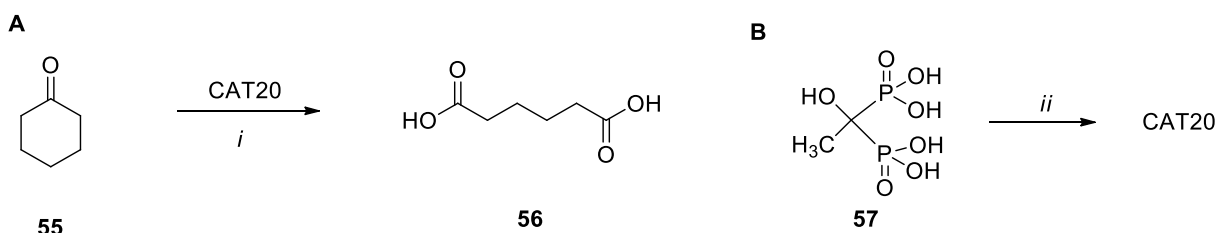


Scheme 14. A. Oxidation or hydrocarboxylation of cycloalkanes **51** catalyzed by CAT19; B. The structure of CAT19. Reaction conditions: *i.* **51** (1mmol), CO (2 MPa), $\text{K}_2\text{S}_2\text{O}_8$ (1.5 mmol), CAT19 (1 μmol), $\text{CH}_3\text{CN}/\text{H}_2\text{O}$, 60 °C, 3h; *ii.* **51** (2 mmol), H_2O_2 (10 mmol, 50% in H_2O), CAT19 (1 μmol), $\text{CH}_3\text{CN}/\text{H}_2\text{O}$, 50 °C, 3h.

As a result, cycloalkanecarboxylic acids **52** (up to 30% yields) or a mixture of cyclic alcohols **53** and ketones **54** (yields 17% to 23%) under mild conditions (50–60 °C, $\text{CH}_3\text{CN}/\text{H}_2\text{O}$) were formed. The physicochemical analyses of the catalyst CAT19 indicated multiple H-bonding interactions leading to a more complex 2D structure. This catalyst also shows moderate proton-conducting properties ($\sigma = 3.65 \times 10^{-6} \text{ S}\cdot\text{cm}^{-1}$).

The application of phosphonate towards green chemistry in organic–inorganic hybrid material was shown by Bhanja *et al.*⁶⁰ Thus, the selective liquid-phase transformation of cyclohexanone **55** to adipic acid **56** (O_2 , H_2O , atm. pressure) using the hybrid iron(II/III)-phosphonate catalyst derived from etidronic acid **57**, was reported (Scheme 15 A). Metal phosphonate CAT20 ensures high selectivity (96%), and good substrate conversion (72%). The designed catalyst was obtained using 1-hydroxyethylidene-1,1-diphosphonic acid **57**

(FeCl₃, pH 6, Δ, 180 °C, 3 days) (Scheme 15 B), and has been thoroughly characterized by various techniques and crystal-structure determination (BET surface area 236 m² g⁻¹, pore volume of 0.229 cm³ g⁻¹).

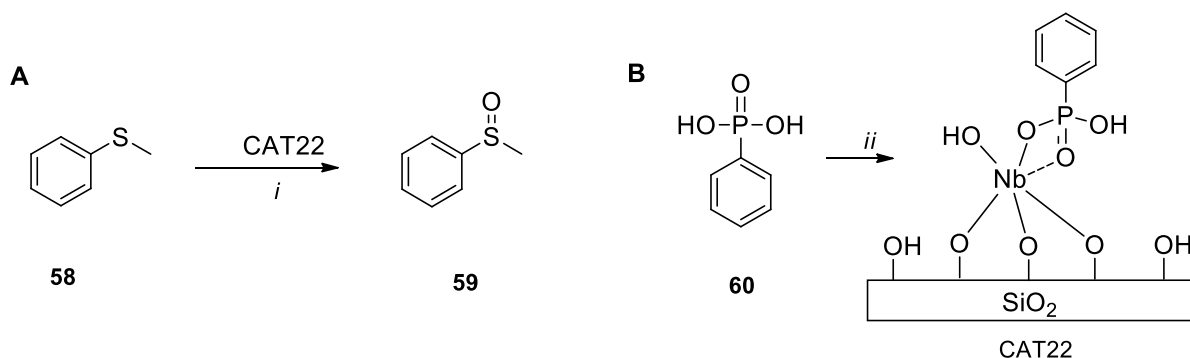


Scheme 15. A. Oxidation of cyclohexanone **55** catalyzed by CAT20; B. The synthesis of CAT20. Reaction conditions: *i.* **55** (5.0 mmol), CAT20 (25 mg), O₂, H₂O, 75 °C, 10h; *ii.* **57** (3 mmol, 60% in H₂O), FeCl₃ (6 mmol), H₂O, NH₄OH to pH 6, 180 °C, 3d.

Phosphonate-containing catalysts have also been used in oxidation reactions. In 2013, Mo *et al.* presented a novel organic-inorganic hybrid material (**ZrNCP**) with formula Zr₅(HPO₄)₆[O₃PCH₂N(CH₂CH₂COOH)CH₂PO₃] which has been used in the synthesis of catalyst CAT21 applied in aldehyde oxidations.⁶¹ The presence of the catalyst allowed the formaldehyde oxidation to formic acid with 90% yield. **ZrNCP** was obtained by combining ZrOCl₂ × 8H₂O, β-alanine-*N,N*-dimethylidenephosphonic acid (ADMPA) and phosphoric acid. To get the final material CAT21 [**ZrNCP-Fe(III)**], it was necessary to introduce Fe³⁺ ions into the layered structure with Fe(NO₃)₃ × 9H₂O. Moreover, it was demonstrated that the coordination of an Fe³⁺ ions *via* nitrogen and carbonyl groups from **ZrNCP** increased the catalytic activity of the prepared hybrid material significantly.

Thornburg *et al.* reported examples of selective catalytic oxidations of thioether **58** to sulfoxides **59** with H₂O₂ (Scheme 16 A).⁶² The authors demonstrated the application of catalyst CAT22 (PPA-Nb-SiO₂), formed by modification of Nb-SiO₂ material with phenylphosphonic acid **60** (PPA) at 65 °C (Scheme 16 B).

Additionally, the catalytic studies of *cis*-cyclooctene epoxidation (as co-reactant in the batch), proved that PPA inhibits direct cyclohexene epoxidation pathways, and sulfoxide is mainly formed, even in the presence of stoichiometric amounts of alkenes.

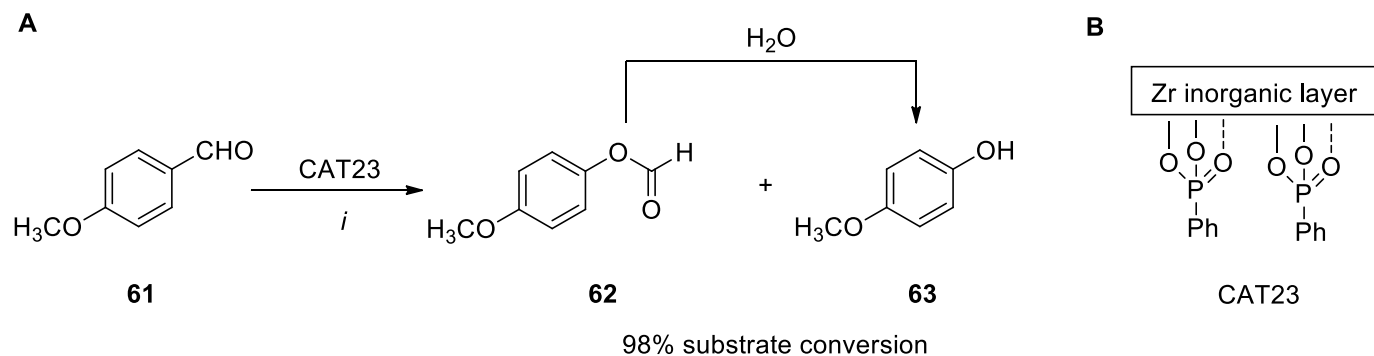


Scheme 16. A. Oxidations of thioether **58** to sulfoxides **59** catalyzed by CAT22; B. The synthesis of CAT22. Reaction conditions: *i.* **58**, CAT22, H₂O₂, CH₃CN, 45 °C; *ii.* **60** (1 eq.), Nb-SiO₂, (1 eq.), CH₃CN, 65 °C, 2h.

The observed selectivity of this reaction most probably resulted from the preferential binding of a Lewis base such as P=O in CAT22 to thioether **58** and product **59**, preventing further oxidation to the sulfone. The

presented studies announced the development of modified-**60** catalysts toward commercially relevant applications.

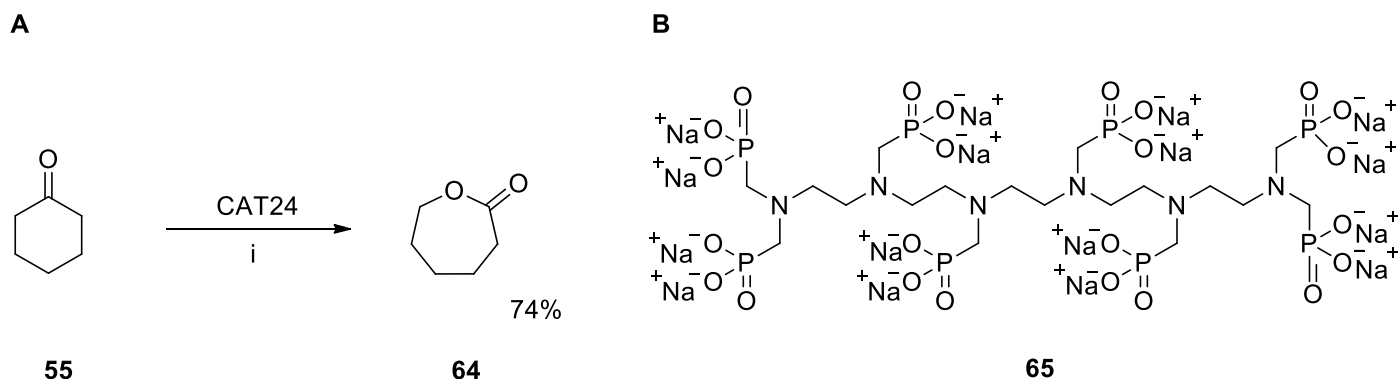
A popular oxidation reaction based on carbon-to-oxygen migrations is the Baeyer-Villiger (BV) rearrangement of ketones or aldehydes with peroxyacids or other peroxy compounds in the presence of acid catalysts. One of the exemplary works is an article of Rocha *et al.* regarding the use of metal phosphonate – zirconium phenylphosphonate amorphous CAT23 [$Zr(O_3PC_6H_5)_2$, (**ZrPPA**)] in the BV oxidation of *p*-methoxybenzaldehyde **61** in the presence of an aqueous solution of hydrogen peroxide and glacial acetic acid (Scheme 17 A).⁶³ The reaction involves the formation of a formate ester **62** which, under aqueous acidic conditions, is hydrolyzed to the target phenol **63** with a quantitative yield.



Scheme 17. A. Baeyer-Villiger oxidation of *p*-methoxybenzaldehyde **61** catalyzed by CAT23; B. Schematic representation of CAT23. Reaction conditions: *i.* **61** (2 mmol), H_2O_2/H_2O (30%, v:v; 8 mmol), AcOH (4 mL), CAT23 (0.1 g), 45 °C, 6h.

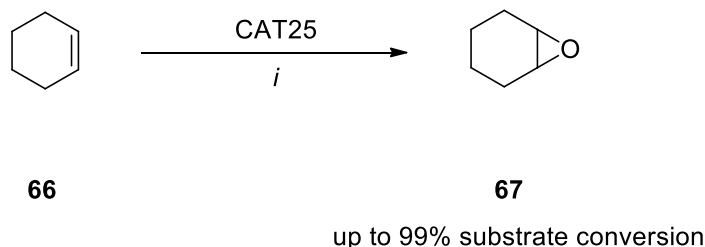
CAT23 (Scheme 17 B) was obtained by mixing an aqueous solution of $ZrOCl_2 \times 8H_2O$ with phenylphosphonic acid (PPA). According to the reaction mechanism, the intermediate species approach the interlayers of CAT23, resulting in greater availability for hydrolysis of **62** to get **63**. The metal-phosphonate catalyst ensure over 90% of the substrate conversion and 100% selectivities to *p*-methoxyphenol **63**, while an analogous reaction, without a catalyst, led to 75% substrate conversion and yielded ester **62**.

Another intriguing example is the work of Dutta *et al.*, which used hybrid porous tin(IV) phosphonate CAT24 (**HMSnP**) for the oxidation of cyclohexanone **55** to adipic acid **64** under liquid-phase conditions (Scheme 18 A).⁶⁴ The synthesis was carried out using molecular oxygen (a balloon filled with air) instead of the H_2O_2 typical in BV oxidation. In addition, a large adsorption capacity of CO_2 on the surface of CAT24 was indicated. A synthesized-by-surfactant-templating method hybrid material was obtained in the reaction of pentaethylenhexamine-octakis-(methyl phosphonic acid)hexadecasodium salt **65** (Scheme 18 B) and quaternary ammonium surfactant – cetyl trimethylammonium bromide (CTAB) followed by the addition of $SnCl_4 \times 5H_2O$, after stirring for 12h. The final material was subjected to hydrothermal treatment at 393K for 48 h. The catalyst can be reused in five reaction cycles without a significant decrease of activity.



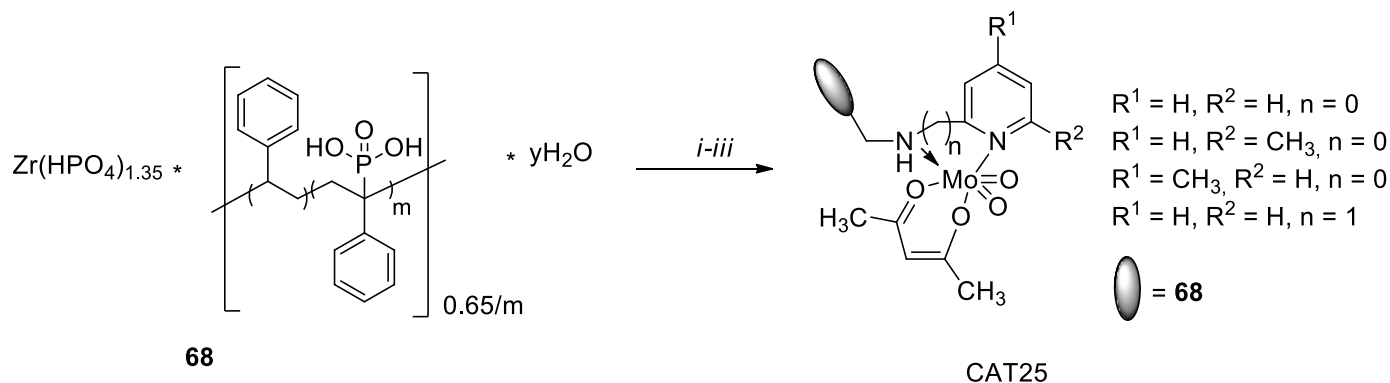
Scheme 18. A. Oxidation of cyclohexanone **55** to adipic acid **64** catalysed by CAT24; B. Organophosphorus precursor **65** used for the synthesis of CAT24. Reaction conditions: *i.* **55** (5.1 mmol), H₂O, 80 °C, 15min, next CAT24 (0.025 g), 80 °C, 5h, balloon filled with air.

Epoxidation is the reaction that has the broadest utility. The addition of oxygen to alkenes yielding epoxide is frequently done using a number of peroxyacids.⁴⁸ Phosphonate ligands are also used in the synthesis of epoxidation catalysts. The epoxidation of cyclohexene **66** to cyclohexene oxide **67** (Scheme 19) was verified in reactions catalyzed by immobilized homogeneous molybdenum catalysts anchored on polymer-inorganic zirconium phosphonate-phosphate (**ZPS-PVPA**), functionalized by various pyridines (CAT25).⁶⁵



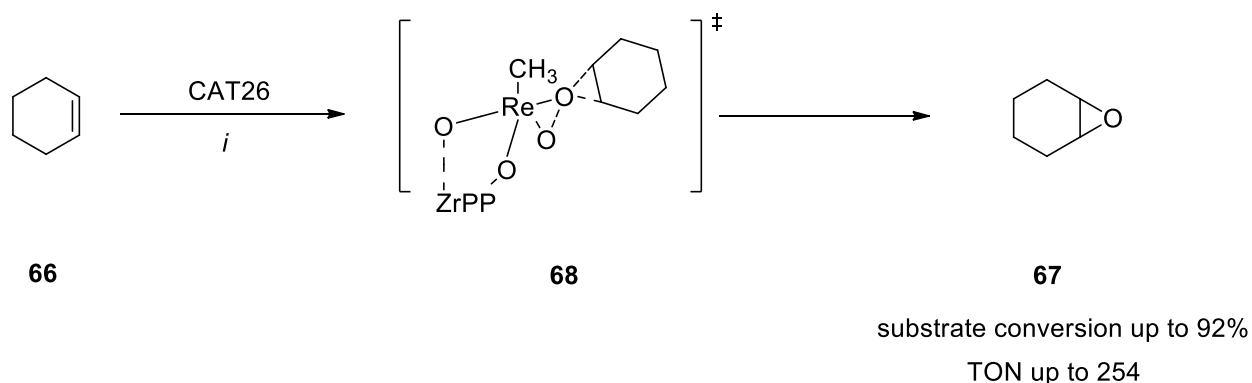
Scheme 19. Epoxidation of cyclohexene **66** catalyzed by CAT25. Reaction conditions: *i.* **66** (1 mmol), TBHP (2 mmol), CAT25 (2 mmol %), *n*-nonane (internal standard, 1 mmol), 1,2-dichloroethane, reflux, 1-6h, N₂.

The results have confirmed 99% substrate conversion in laboratory and industrial scales. Moreover, catalyst CAT25 can be recycled and reused in the reaction for up to 9 runs. The catalyst support **68** (**ZPS-PVPA**) was obtained by reacting styrene-phenylvinylphosphonic acid copolymer (PS-PVPA) with ZrOCl₂ × 8H₂O and sodium orthophosphate. Next, addition of chloromethyl-methyl ether and anhydrous zinc chloride resulted in the formation of chloromethyl-zirconium poly(styrene-phenylvinylphosphonate)-phosphate (**ZCMPS-PVPA**), which was modified with pyridine groups. On such a prepared hybrid material, the immobilization of molybdenum originating from MoO₂(acac)₂ led to CAT25 (Scheme 20).



Scheme 20. Synthesis of CAT25. Reaction conditions: *i.* **68** (8.55 mmol), chloromethyl methyl ether (9.3 mL), anh. ZnCl_2 (14.18 mmol), 45 °C, 8h; *ii.* ZCMPS-PVPA (5.0 g), toluene, 10 min, RT, then pyridine, 80 °C, 12h; *iii.* EtOH, RT, 30 min, then $\text{MoO}_2(\text{acac})_2$, 60 °C, 24h.

Another example of the attractive application of phosphonate-supported catalysts is proposed by He *et al.*, i.e., the epoxidation of cyclohexene **66** to epoxide **67** via transition state **68** (Scheme 21). The reaction was carried out in the presence of the urea-hydrogen peroxide (UHP) adduct as an oxidizing agent.⁶⁶ The epoxidation catalyst CAT26 (**MTO/ZrPP**) was based on methyltrioxorhenium anchored onto zirconium phenylphosphonate (**ZrPP**), which was obtained by mixing $\text{ZrOCl}_2 \cdot 8\text{H}_2\text{O}$, hydrofluoric acid and phenylphosphonic acid (PPA). Methyltrioxorhenium (MTO) was then immobilized by conventional impregnation on the support surface.



Scheme 21. Epoxidation of cyclohexene **66** catalyzed by CAT26. Reaction conditions: *i.* **66** (9.8 mmol), UHP (19.2 mmol), CAT26 (0.1 g), MeOH, RT, 6h.

The asymmetric epoxidation of α -methylstyrene was examined using chiral (salen)Mn(III) complexes anchored on sulfoalkyl-modified zirconium poly(styrene-isopropenyl phosphonate)-phosphate CAT27 (**ZPS-IPPA**).⁶⁷ The catalysts, and the influence of various supporting linkage lengths were verified in the presence of sodium hypochlorite (NaClO) and 4-phenyl-pyridine N-oxide (PPNO). In addition, it was reported that the catalyst can be recycled and used in 5 runs without significant loss of substrate conversion or *ee* value. It was the first such example of a salen-type complex that was immobilized by axial coordination.

CAT27 (Figure 5) was synthesized by mixing a linear polystyrene-isopropenyl phosphonic acid (**PS-IPPA**) copolymer, hydrated sodium orthophosphate, and $\text{ZrOCl}_2 \cdot 8\text{H}_2\text{O}$.⁶⁸ The final hybrid material was obtained by immobilization of the Jacobsen catalyst into **ZPS-IPPA**.

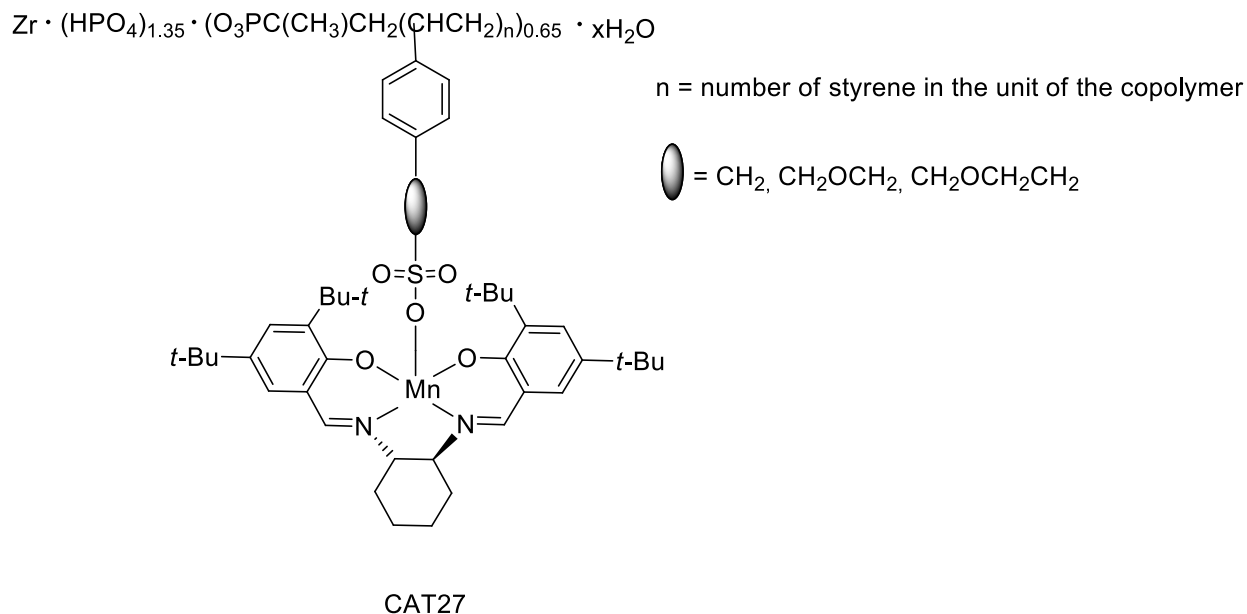
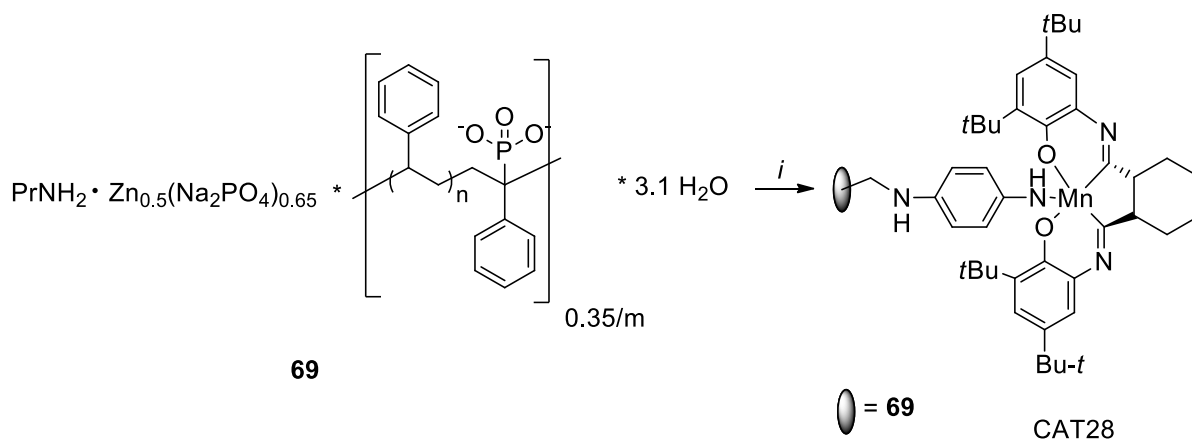


Figure 5. The structure of CAT27.

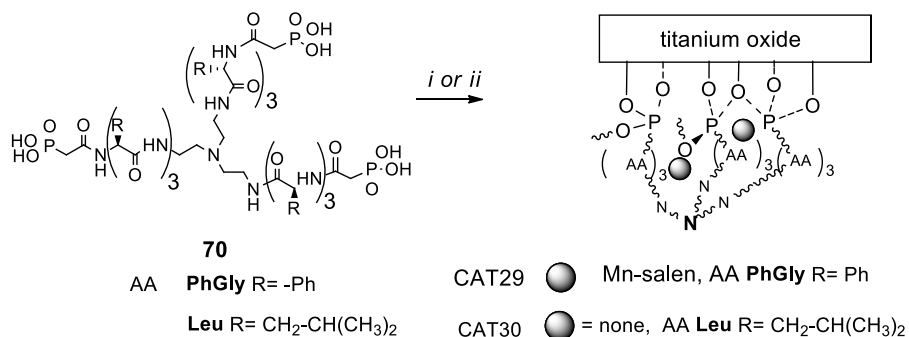
The (salen)Mn(III)-grafted catalysts on phosphonate-containing crystalline-layered organic polymer-inorganic hybrid materials have been used to study catalytic asymmetric epoxidation of α -methylstyrene or indene by Huang *et al.*⁶⁹ The applied hybrid materials **69** were based on zinc poly(styrene-phenylvinylphosphonate)-phosphates and different amines were used as templates e.g., propylamine (PA) (Scheme 22). Next, **69** was modified with *p*-phenylenediamine and the chiral (salen)Mn(III) was immobilized, to give effective and stable CAT28. Moreover, due to mesoporous structure of polymer and support pore size in this type of organic-inorganic hybrid material, the enhancement of catalytic activity was observed.



Scheme 22. Synthesis of CAT28 containing chiral salen Mn(III). Reaction conditions: *i.* **69** (0.59 mmol), $\text{CH}_3\text{OCH}_2\text{Cl}$ (1.6 mL), ZnCl_2 (4.2 mmol), next *p*-phenylenediamine, Na_2CO_3 (0.01 mol), CuI (1 mmol), alcohol (50 mL); then salen Mn(III)Cl (4 mmol), TEA (5 mmol), THF, reflux, 10h.

The enantioselective epoxidation of styrene and its derivatives (Table 5) was studied with the application of the heterogeneous titanium-phosphonate material containing chiral tripodal-architecture-origin amino acids such as phenylglycine (**TiP-PhGly**) with encapsulated achiral (salen)Mn(III) - CAT29.⁷⁰ In this case, the synthesis

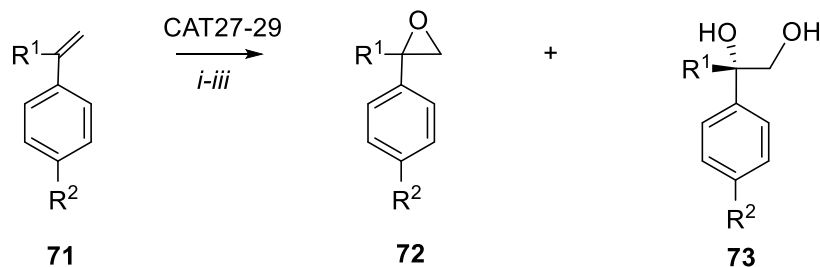
of the peptidic catalyst involved coupling of the amino acids (PhGly) to tris(2-aminoethyl)amine, followed by introduction of the phosphonoacetic acid moieties to get tripodal **70**. Subsequent reaction of **70** with $\text{Ti}(\text{O-}i\text{-Pr})_4$, and encapsulation of the achiral (salen)Mn(III), gave CAT29 (Scheme 23). Analogous application of leucine (Leu) instead of phenylglycine (PhGly) in **70**, and subsequent treatment with $\text{Ti}(\text{O-}i\text{-Pr})_4$, led to CAT30, possessing enantioselective catalytic activity verified in epoxide ring opening reactions.⁷¹ The application of this particular catalyst will be discussed in section concerning acid-promoted reactions.



Scheme 23. Synthesis of peptidic catalysts on titanium oxide CAT29 – CAT30; Reaction conditions: *i.* **70** R = Ph, Mn(III)-salen, $\text{Ti}(\text{O-}i\text{-Pr})_4$; *ii.* **70** R = $\text{CH}_2\text{-CH}(\text{CH}_3)_2$, $\text{Ti}(\text{O-}i\text{-Pr})_4$, DMSO, RT.

The results concerning asymmetric epoxidation of styrene or α -methylstyrene **71** to **72**, performed using catalysts CAT27 – 29 are presented in Table 5. The reaction catalysed by CAT27 was performed in the presence of sodium hypochlorite (NaClO) and 4-phenyl-pyridine N-oxide (PPNO) and led to **72** (48% *ee*) with substrate conversion of 57.6%. As indicated, the obtained enantiomeric excess (*ee*) value for **72** ($\text{R}^1 = \text{CH}_3$, $\text{R}^2 = \text{H}$) was higher after immobilization of (salen)Mn(III) complexes on CAT27 than in the case of the homogeneous Jacobsen catalyst (84%*ee* and 54% *ee*, respectively).⁶⁸ The asymmetric epoxidation of styrene or α -methylstyrene **71** using catalyst CAT28 (5 mol%) and *m*-CPBA/NMO as oxidant systems, was carried out at -20°C in CH_2Cl_2 for 5h to give the α -methylstyrene (or indene) oxides **72** with enantioselectivity 99% *ee* (or 88% *ee*), and substrate conversion of 99% (or 96%).⁶⁸ The stereochemistry of **72**, however, has not been indicated.

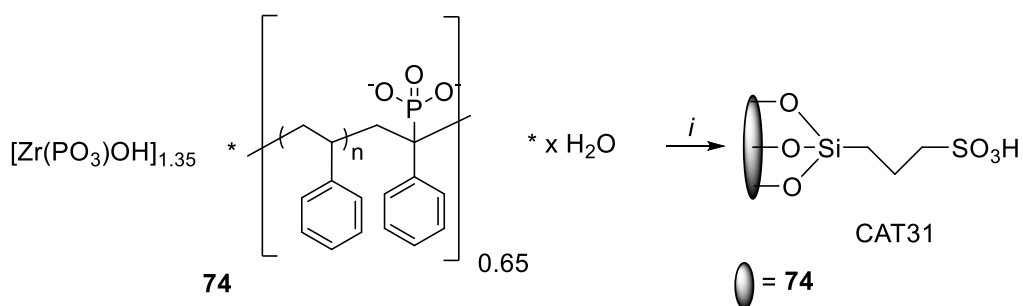
For comparison, the reaction catalyzed by CAT29 with aqueous hypochlorite in THF led to **71** with a substrate conversion from 17 - 86%.⁷⁰ Additionally, the formation of glycols **73** resulting from epoxide ring opening, with selectivity from 20-65%, and enantioselectivity >99% was observed. The *S* isomer was the major isomer in all cases.

Table 5. Epoxidation of styrenes **71** catalyzed by CAT27 – CAT29 and hydration of epoxide catalyzed by CAT29

Substituents	Catalyst	Epoxide 72 selectivity; % <i>ee</i>	Diol 73 selectivity ^a	Conversion of 71 [%]
R ¹ = H, R ² = H	CAT27	>99; 48 ^b	0	57.6
R ¹ = CH ₃ , R ² = H	CAT27	>99; 84 ^b	0	70.1
R ¹ = CH ₃ , R ² = H	CAT28	>99; 99.5 ^b	0	99.2
R ¹ = H, R ² = H	CAT29	25; 36 ^c	65 ^d	17
R ¹ = H, R ² = CH ₃	CAT29	35; 7 ^c	20 ^d	84
R ¹ = CH ₃ , R ² = H	CAT29	15; 10 ^c	40 ^d	20
R ¹ = CH ₃ , R ² = CH ₃	CAT29	25; 5 ^c	25 ^d	86

Reaction conditions: *i.* **71** (1 mmol), nonane (1 mmol), CAT27 (3 mol%), NaOCl in buffered solution (pH 11.3, 0.55M), PPNO (0.38mmol), CH₂Cl₂, 20 °C, 24h; *ii.* **71** (1 mmol), NMO (5 mmol), *m*-CPBA (2 mmol), CAT28 (5 mol %), CH₂Cl₂, -20 °C, 5h; *iii.* **71** (0.1 mmol), NaOCl in buffered solution (0.2 mmol), CAT29 (10 mg), THF, 3 °C, 48h. ^a % *ee* >99, in each case; ^b the stereochemistry is not indicated; ^c The major isomer is *S*; ^d The *S* isomer.

The epoxidation of vegetable oils is also exceptionally attractive due to the potential use of the products as stabilizers of polyvinyl chloride. Examples of such epoxidation using organophosphonate catalysts are also known. In 2019, Zou *et al.* described a novel solid acid catalyst CAT31 based on zirconium poly(styrene-phenylvinyl-phosphonate)-phosphate **74** (ZPS-PVPA).⁷²

**Scheme 24.** Synthesis of sulfonic acid-functionalized zirconium poly(styrene-phenylvinyl-phosphonate)-phosphate CAT31.

The final material was obtained via anchoring of the thiol group on **74** $\{[\text{Zr}(\text{PO}_3)\text{OH}]_{1.35}[\text{O}_3\text{PC}(\text{Ph})\text{CH}_2(\text{CHPhCH}_2)_n]_{0.65} * \text{xH}_2\text{O}\}$ and thiol oxidation to sulfonic acid. CAT31 showed high

catalytic activity in the epoxidation of soybean oil with TBHP (*tert*-butyl hydroperoxide) as an oxidant. The catalyst could be recycled, and reused in 5 runs without greatly decreasing the substrate conversion.⁷²

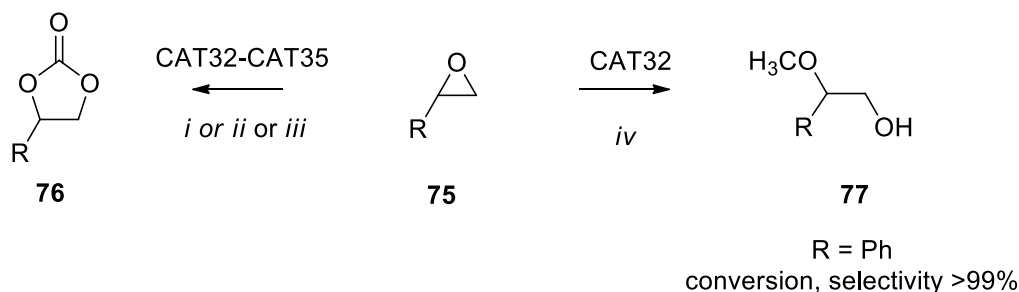
2.4. Cycloaddition of CO₂ to epoxide

Besides asymmetric synthesis, one of the eco-trends in chemistry is the catalytic capture of CO₂,⁷³ which is considered one of greenhouse gases involved in climate warming. As a promising approach, one can envisage the cycloaddition of CO₂ to an epoxide, yielding useful cyclic carbonates.

In view of this topic, the application of a porous copper-phosphonate catalyst was reported by Ai *et al.*⁷⁴ The conversion of small aliphatic as well as aromatic oxiranes **75** to cyclic carbonates **76** in yields of up to 99% was performed in a carbon-dioxide atmosphere and higher pressure (1 MPa), using catalyst CAT32 (at 100 °C) in the presence of TBAB (tetrabutylammonium bromide) as a co-catalyst (Table 6). Furthermore, the copper-phosphonate catalyst CAT32 has proven to be an excellent catalyst in ring-opening reactions of epoxides under ambient conditions, leading to α -methoxyalcohol **77** with 99% conversion, and more than 99% selectivity. This catalyst could be reused in at least 3 cycles in both types of reactions.

For comparison, the analogous cycloadditions of CO₂ to epoxide **75** were performed using Ni phosphonate as catalyst CAT33.⁷⁵ The high catalytic efficiency of CAT33 at CO₂ pressure of 1 MPa, and room temperature, was demonstrated for small-size aliphatic epoxides, e.g., glycidol or epichlorohydrine (99% and 83%, respectively). Analogous reactions of styrene oxide or glycidyl ether **75**, gave carbonates **76** with lower yields, even after 48h (8% or 20%). A similar tendency of the conversion of epoxide **75** to carbonate **76** was observed in the case of the catalytic cycloaddition of CO₂ catalyzed by manganese phosphonate CAT34.⁷⁶ Thus, under the applied conditions of CO₂ (1 MPa), and room temperature, aliphatic oxiranes were efficiently transformed in yields of 77 - 99%, while styrene oxide and glycidyl phenyl ether **75** gave products in yields of 4 - 6%, respectively. Another catalyst used for the CO₂ insertion to epoxides **75** is CAT35 in the form of organic-inorganic iron-phosphonate nanoparticles, presented by Rosati *et al.*⁷⁷ The synthesized CAT35 efficiently catalysed CO₂ cycloaddition to small-aliphatic oxiranes and bigger styrene oxide or phenyl glycidol ether under mild conditions yielding **76** in the range of 88 - 97% (Table 6). The CAT35 was successfully reused in five runs with over 90% substrate conversion.

The authors have proposed a mechanism of **76** formation involving the activation of the epoxide by phosphonic acid moieties and metal centers in CAT32, simultaneously acting as Brønsted and Lewis acids, respectively.⁷⁴ Subsequent nucleophilic attack of Br⁻ (from TBAB) from the less hindered side causing epoxide opening, followed by CO₂ insertion, led to the obtained **76**. What is important is that the CO₂ as well as the oxirane **75** enter and assemble in the porous channels of the catalysts.

Table 6. Cycloaddition using CO₂ to epoxides **75** catalyzed by CAT32 - CAT35, and catalytic epoxide ring opening.

R	CAT32 [%] ^a	CAT33 [%] ^a	CAT34 [%] ^a	CAT35 [%] ^a
CH ₂ OH	99	99	99	97
CH ₂ Cl	99	83	77	88
Ph	99	8	4	97
CH ₂ OPh	99	20	6	96

Reaction conditions: *i.* **75** (20 mmol), CAT32 (2 μmol), TBAB (0.3 mmol), CO₂, 1 MPa, 100 °C. *ii.* **75** (20 mmol), CAT33 (0.05 mol %) or CAT34 (0.02mmol), TBAB (0.3 mmol), CO₂, 1 MPa, RT, 48h or 36h; *iii.* **75** (5 mmol), CAT35 (50mg), TBAB (0.083 mmol), CO₂, 100 MPa, RT, 12h; *iv.* **75** R= Ph (0.2 mmol), CAT32 (2 μmol), 25° C, MeOH ^a yield of **76**.

In the syntheses of the above-described cycloaddition catalysts, various aromatic or aliphatic phosphonic acids as precursors were employed (Figure 6). The copper phosphonate catalyst CAT32 [Cu₇(H₁L)₂(TPT)₃(H₂O)₆] was synthesized by the reaction of tetraphenylsilane tetrakis-4-phosphonic acid **78** (H₈L), Cu(OAc)₂ and a ligand TPT: [5-(4-(1H-1,2,4-triazol-1-yl)phenyl)-1H-tetrazole] in water at 180 °C for 3 d.⁷⁴ The reaction of rigid tetraphosphonic acid **79** (H₈L), nickel(II) nitrate hexahydrate and HF in H₂O/MeOH at 150 °C for 3 d gave catalyst CAT33.⁷⁵ For comparison, the Mn (II) catalyst CAT34 was prepared from pyridin-4-yl phosphonic acid **80** (H₂L) and manganese (II) acetate tetrahydrate in water at 80 °C (3 d).⁷⁶ Additionally, the application of such a phosphonate precursor as hexamethylenediamine- *N,N,N',N'*-tetrakis-(methylphosphonic acid) **81** (HDTMP) in the reaction with an aqueous solution of FeCl₃ at 150 °C for 24h, led to hybrid material CAT35.⁷⁷

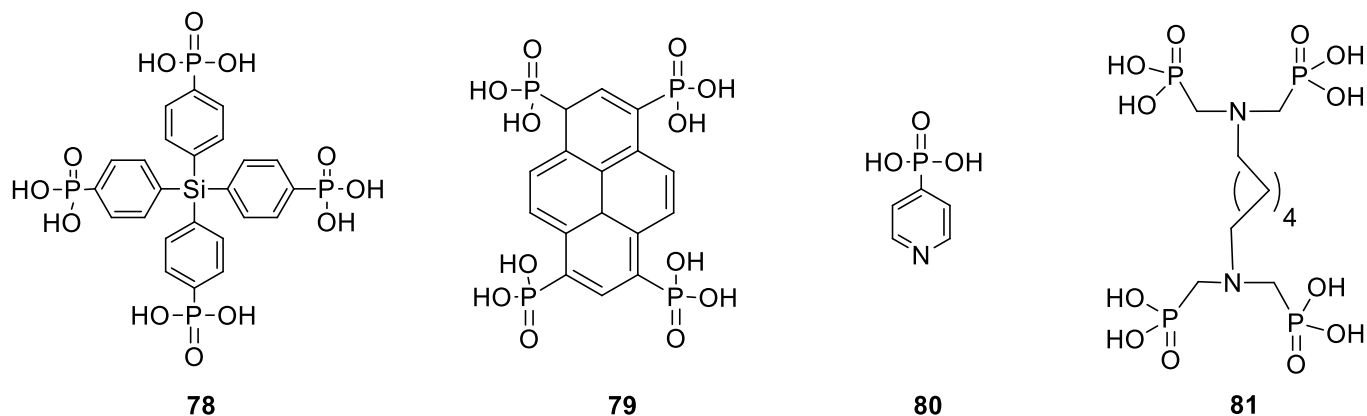


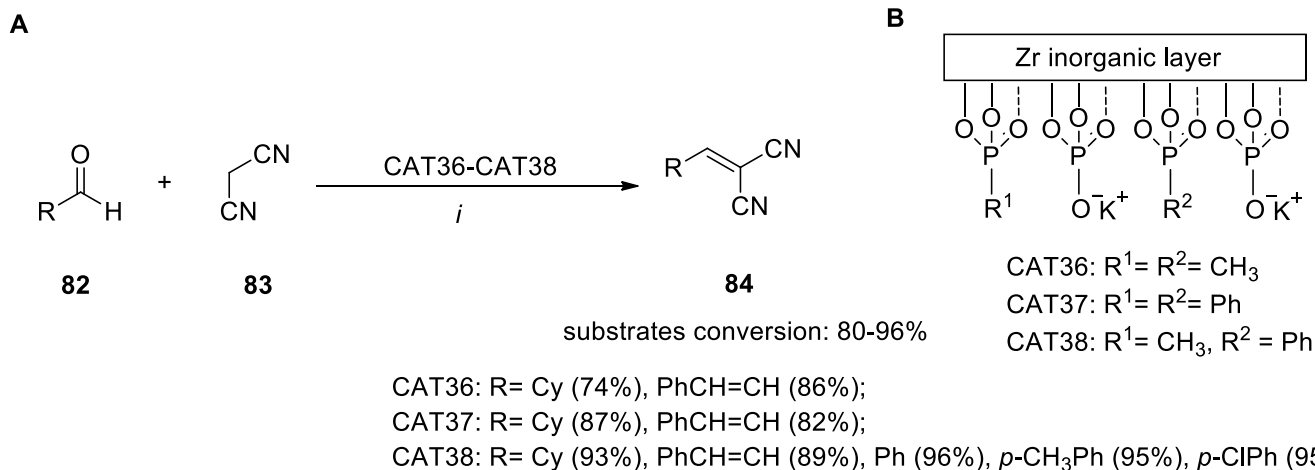
Figure 6. Organophosphorus precursors **78** – **81** used for the synthesis of catalysts CAT32 – 35.

All catalysts were fully characterized by different methods and can be easily separated and reused without significant reduction in the catalytic ability.

2.5. Condensations

Another important class of organic chemistry reactions, in which two or more molecules combine, usually in the presence of a catalyst to form a larger product with a simultaneous loss of water or another small molecules, are condensation reactions. Some of them are catalyzed by acids, although, in the most common condensations, use of a base is necessary.

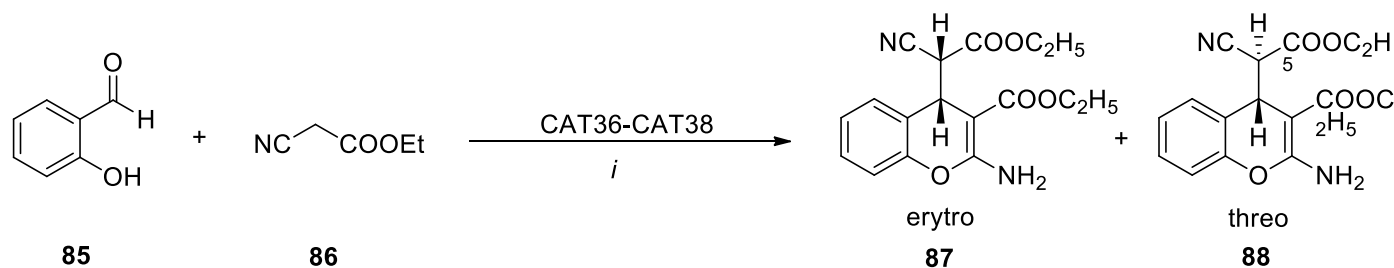
In 2018, Rosati *et al.* described the solid Brønsted bases containing phosphonate groups used in the Knoevenagel condensation.⁷⁸ A condensation has occurred between substituted aldehydes **82** and malononitrile **83** (Scheme 25 A), while as catalysts, zirconium potassium phosphate/phosphonates (CAT36 – CAT38, **ZrKPs**) (Scheme 25 B) were used. Moreover, the reactions did not require the use of organic solvents. The applied catalysts could be recycled and showed high activity in 5 reaction cycles without structural changes (substrate conversion up to 99%, isolated yields of **84** up to 96%).



Scheme 25. A. Knoevenagel condensation of aldehydes **82** with malononitrile **83** catalyzed by CAT36 – CAT38; B. Schematic representation of CAT36 – CAT38. Reaction conditions: *i.* **82** (1 mmol), **83** (1 mmol), CAT36 – CAT38 (2 mol %), RT, 1h. ^a isolated yield of **84**.

The catalysts have also been used successfully in Knoevenagel condensation of salicylaldehyde **85** with ethyl cyanoacetate **86** to give biologically important 2-amino-4*H*-chromene (**87**, **88**). The product was obtained in the form of two diastereoisomers in which the predominant form was the *erythro* isomer **87** (Table 7). In addition, it was noted that compound **87** left in the CDCl₃ solution epimerizes to the *threo* isomer **88** (**87**:**88** = 80:20 after 6 h).⁷⁸

Table 7. Knoevenagel condensation of salicylaldehyde **85** with ethyl cyanoacetate **86** catalyzed by CAT36 – CAT38

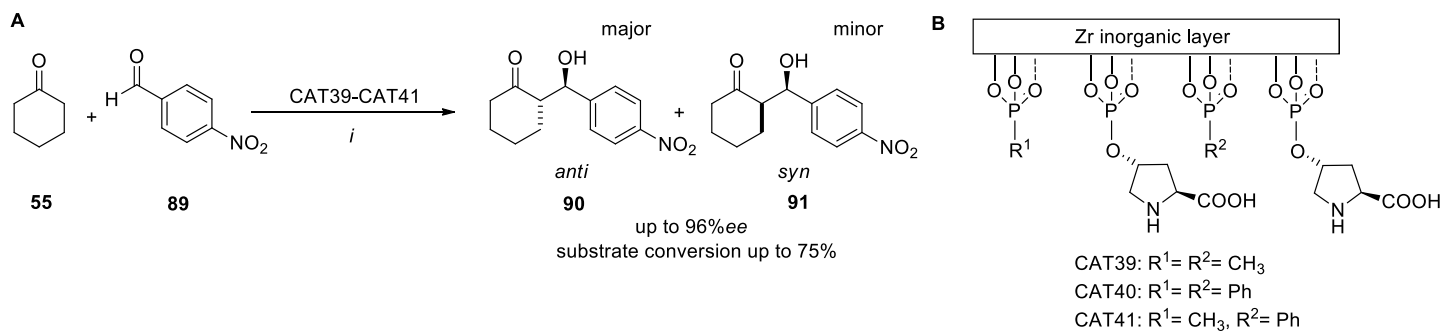


	CAT36 [%]	CAT37 [%]	CAT38 [%]
Substrat conversion [%]	99	99	99
Isolated yield [%]	92	94	93
87/88	97/3	99/1	99/1

Reaction conditions: *i*. **85** (1 mmol), **86** (2 mmol), CAT36 – CAT38 (5 mol %), 50 °C, 4h.

Amorphous solids (CAT36 – CAT38, Scheme 25 B) were obtained in the reaction of ZrOCl₂ × 8H₂O with a phosphorus source – phosphoric acid and methyl and/or phenylphosphonic acid (P/Zr=3 ratio). The obtained zirconium phosphate/phosphonates (**ZrHPs**) were then treated with a solution of *t*-BuOK. Analogous use of KOH causes changes of the layer composition, and, consequently, decreases the catalyst effectiveness, which was confirmed by ³¹P NMR analysis. It has been shown that the methyl and phenyl groups present on the catalyst layer caused the formation of larger dimension pores, and also influence higher catalytic activity compared to inorganic Zr(KPO₄)₂.⁷⁸

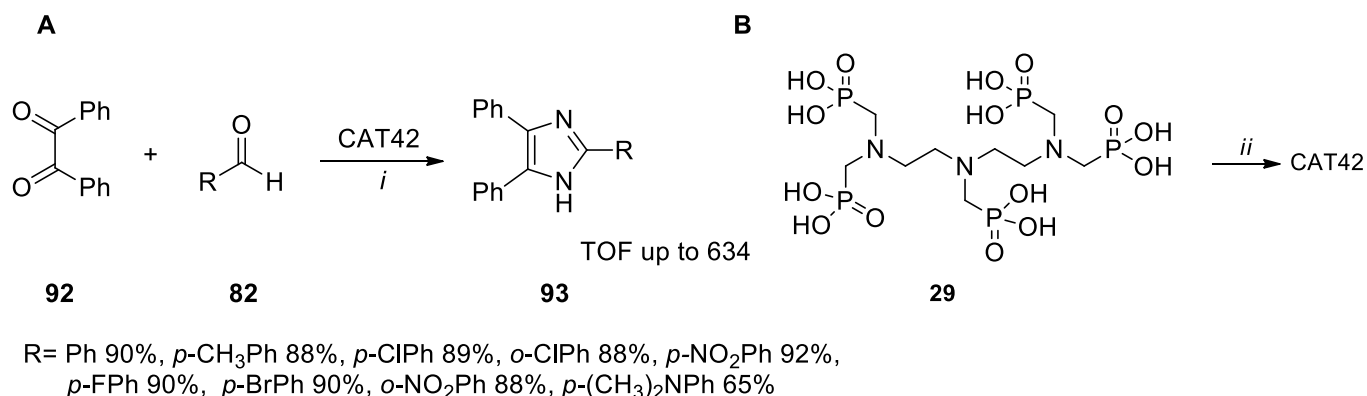
The above catalysts are an extension of the work of the previously investigated use of zirconium phosphates and methyl and/or phenyl phosphonates-supported *L*-proline. In 2011, Calogero *et al.* published a study concerning solid catalysts functionalized by a chiral ligand.⁷⁹ The obtained materials showed high catalytic activity in the asymmetric aldol reaction of cyclohexanone **55** with *p*-nitrobenzaldehyde **89** (Scheme 26 A). The results confirmed that a presence of the chiral ligand on the surface has an effect on increasing catalytic activity. *L*-Proline covalently linked with zirconium material ensured a high diastereoselectivity of the reaction, and a large enantiomeric excess (**90/91** ratio up to 94:6 and up to 96% *ee*). The reaction can be carried out both in a mixture of DMF and water (9:1) and the more eco-friendly condition, i.e., solely water.



Scheme 26. A. Aldol reaction of cyclohexanone **55** with *p*-nitrobenzaldehyde **89** catalyzed by CAT39 – CAT41; B. Schematic representation of CAT39 – CAT41. Reaction conditions: *i.* **55** (0.625 mmol), **89** (0.125 mmol), CAT39 – CAT41 (0.062 mmol, 0.0375 mmol of P-Prol groups – 30 mol %), DMF/H₂O (9:1, v:v) or H₂O, 30 °C, 4 d.

In order to prepare the catalysts CAT39 – CAT41, *trans*-4-hydroxy-*L*-proline was mixed with phosphorus oxychloride to get (4*R*)-4-phosphonoxy-*L*-proline. In the next step, the obtained amino acid was immobilized on an inorganic zirconium layer by the reaction with an aq. solution of ZrOCl₂ and methyl and/or phenylphosphonic acids (P/Zr=3 ratio) (Scheme 26B). The solid materials obtained were fully characterized by NMR spectroscopy, TG DTA, ICP-OES and nitrogen adsorption-desorption isotherms.⁷⁹

Organic phosphonate ligands have also found application in the synthesis of an organic-iron nanocatalyst CAT42 (**Fe-DTPMP**) which catalyzed a tri-component condensation reaction. In 2020, Arpanahi *et al.* presented a novel organic-inorganic hybrid catalyst based on the ligand, diethylenetriamine penta(methylene phosphonic acid) (DTPMP) **29**.⁸⁰ The described catalyst showed high activity in condensation reactions between aromatic aldehydes **82**, 1,2-diphenyl-1,2-ethanedione **92**, and ammonium acetate to 2,4,5-trisubstituted imidazoles **93** (Scheme 27 A).

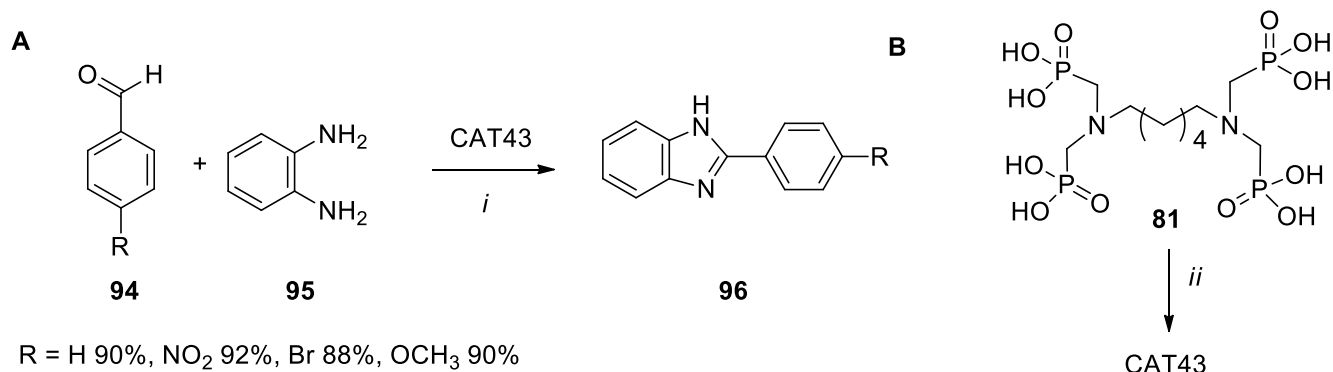


Scheme 27. A. Tri-component condensation of aromatic aldehydes **82** and 1,2-diphenyl-1,2-ethanedione **92** catalyzed by CAT42; B. The synthesis of CAT42. Reaction conditions: *i.* **92** (1 mmol), **82** (1 mmol), NH₄OAc (3 mmol), CAT42 (0.05 g), 100 °C, 1h; *ii.* FeCl₂ (50 mL, 0.25 M), CTAB (1.5 g), 30 °C, 1h, next **29** (25 mL, 0.1 M), NH₃ to pH= 9, 75 °C, 6h.

The authors found that the yields of the heterocyclic compounds were influenced by the substituent from the aromatic ring of the aldehyde. The presence of an electron-withdrawing substituent increases the yield of compound **93** while the opposite effect was observed for an electron-donating group. The tested catalyst provided a short reaction time and the possibility of reuse in 4 runs. Moreover, the reaction did not require the

use of solvents. The described hybrid CAT42 was synthesized by mixing iron (II) chloride (aq. solution) with a surfactant, cetrimonium bromide (CTAB). Then the phosphonate ligand **29** was added, and the reaction mixture was treated with ammonia to pH= 9 (Scheme 27 B). After drying, the precipitated solid was characterized using a number of structural analyses, including FT-IR, TGA, XRD, BET and others.⁸⁰

For comparison, the condensation of various aromatic aldehydes **94** with *o*-phenylenediamine **95** using an organic–inorganic hybrid porous iron–phosphonate CAT43 gave the benzimidazole derivatives **96** in yields ranging from 30-92% (Scheme 28A). This catalyst was synthesized from hexamethylenediamine-*N,N,N',N'*-tetrakis-(methylphosphonic acid) **81** (HDTMP) and FeCl₃ under different hydrothermal conditions (Scheme 28B), and possessed structures of nanoparticles or nanorods or flake-like morphology.⁸¹



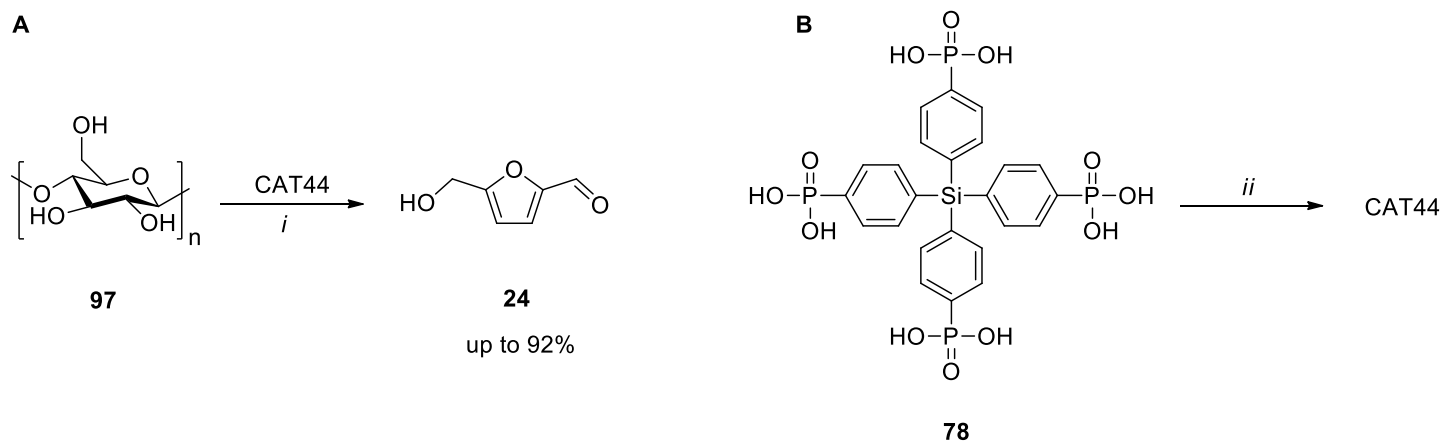
Scheme 28. A. Condensation of aromatic aldehydes **94** and *o*-phenylenediamine **95** catalyzed by CAT43; B. The synthesis of CAT43. Reaction conditions: *i*. **94** (1 mmol), **95** (1 mmol), CAT43 (30 mg), EtOH (5ml), 298K, 2-3h; *ii*. FeCl₃(10 mol), H₂O (10g) then **81** (2.54 mol, 25%), 423K or 443K or 453K, 24h.

The authors proposed a mechanism involving activation of the carbonyl group in aldehyde **94** by the iron center in the catalyst CAT43, followed by attack of the amine group in **95**, with the tertiary amine group in the catalyst facilitating elimination of a water molecule to give product **96**.

2.6. Other acid-promoted reactions

Most organic reactions occur under acidic conditions. In this part, the application of the Brønsted acidity of the catalyst in organic reactions will be discussed.

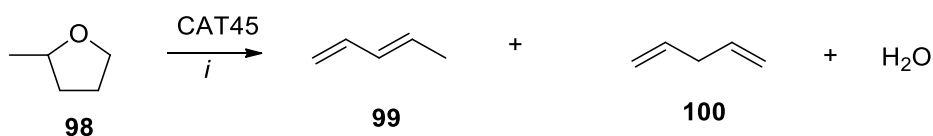
Phosphonate-based catalysts are used especially for the conversion of biomass into green chemicals or fuels. An intriguing example of this topic is the work of Liu *et al.* from 2020 in which the authors presented three-step transformations of saccharides catalyzed by a cobalt-phosphonate CAT44 [Co₂(2,2'-bipy)(H₄L)(H₂O)]H₂O catalyst.⁸²



Scheme 29. A. Transformation of cellulose **97** to HMF **24** catalyzed by CAT44; B. The synthesis of CAT44. Reaction conditions: *i.* **97** (200 mg), NaCl (sat.), CAT44 (20 mg), methyl isobutyl ketone, 2-butanol, 200 °C, 1h; *ii.* Co(NO₃)₂ (0.08 mmol), **78** (0.04 mmol), 2,2-bipyridine (0.04 mmol), H₂O, 180 °C, 3 d.

The authors found that the catalyst allowed the formation of hydroxymethylfurfural HMF **24** from cellulose **97** *via* hydrolysis to glucose. Subsequent glucose isomerization to fructose, and dehydration of fructose yielded **24** (intermediate products confirmed by GC-MS analysis). Starting from cellulose, it is possible to obtain HMF **24** in up to 92% yield (Scheme 29 A). The final yield of **24** was influenced by the weight percent of the catalyst CAT44 and the type of cellulose used (10 wt% CAT44; microcrystalline **97** = 33%; regenerated **97** = 50%, 40 wt% CAT44, regenerated **97** = 59%). The applied catalyst combines two types of acidity, Brønsted acid (phosphonic acid, **78**) responsible, among others, for the cellulose hydrolysis, and Lewis acid (cobalt ion as a metal centre) responsible for the glucose to fructose isomerization. The catalyst obtained in hydrothermal reaction of **78** with Co(NO₃)₂ and 2,2-bipyridine (Scheme 29 B), was successfully reused in 4 runs.⁸²

Another studied reaction relying on the Brønsted acidity of the obtained catalyst CAT45 pertained to the conversion of 2-methyl-tetrahydrofuran **98** (2-MTHF) into two pentadiene PD isomers, **99** and **100** (1,3 and 1,4PD). Thus, a one-pot dehydration and decyclization reaction, with the application of a phosphonate-modified material based on a metal-organic framework with UiO-66 topology (CAT45), was demonstrated (Scheme 30).⁸³ The authors reported low and moderate, site-time-dependent yields (~ 23%) in the case of the **98** conversion, and, at the same time, high selectivity to pentadienes (~ 90% on a per C basis), i.e., 22% of **99** and 67% of **100**.

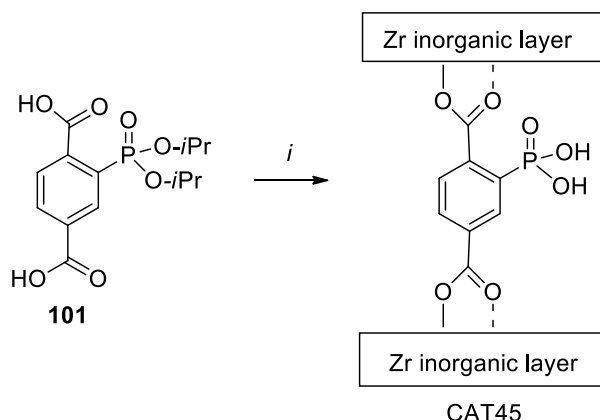


Scheme 30. Tandem dehydration/decyclization reaction of 2-methyl-tetrahydrofuran **98** catalyzed by CAT45; Reaction conditions: *i.* **98**, CAT45 (0.05 g), 653 Pa, 280 °C, weight hourly space velocity (WHSV) 0.31 h⁻¹.

Moreover, CAT45's weak Brønsted acidity was confirmed by the dehydration of *i*-PrOH in comparison to ethanol, and Hoffman elimination of *tert*-butylamine.

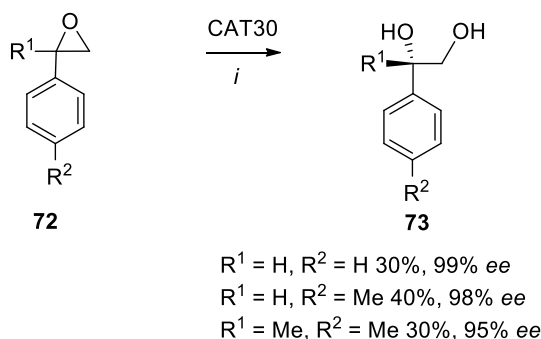
Synthesis of the MOF-derived catalyst CAT45 involves post-synthetic modifications (PSM) of UiO-66's well-defined sites with 2-diisopropylphosphono-terephthalic acid **101** as a phosphorus source, by a solvent-assisted ligand exchange method (in KOH/THF). Next, acid treatment (1M HCl, AW), to deprotect the

phosphonate isopropyl groups gave the possibility of distribution of acid sites throughout the framework (Scheme31). The catalyst has the majority of P-OH bonds with small or no interactions with the zirconium cluster. The catalyst CAT45 (P-UiO66-AW) has also shown high selectivity in three consecutive reaction-regeneration cycles.⁸³



Scheme 31. The synthesis of CAT45. Reaction conditions: *i.* **101**, KOH_{aq}/THF, then UiO-66, 180 °C, 5 d, next HCl, 100 °C, 12h, then activation 120 °C, 20h.

The interesting example of the application of homochiral titanium phosphonate on a polypeptide scaffold to catalyze diols formation *via* epoxide opening in an asymmetric manner, was reported by Milo *et al.*⁷¹ Thus, the enantioselective water addition to racemic styrene oxide and its derivatives **72** was studied with the application of the heterogenous catalyst containing leucine CAT30.⁷⁰ The studied reactions resulted in (*S*)-diols **73** with 20 - 30% yields, and 95 - 99% *ee* (Scheme 32).



Scheme 32. Enantioselective hydration of styrene oxide **72** derivatives catalyzed by CAT30. Reaction conditions: *i.* (*R/S*)-**72** (20 mL), THF/H₂O, pH 7 or 11 (buffer) CAT30 (10 mg), 38 °C, 72h.

In this particular example, authors proposed the mechanism involving the activation of oxirane by a partially positively-charged peptide yielding carbocation. Next, the enantioselective attack of water directed by homochiral catalyst led to (*S*)-diol.⁷¹ It is worth noting that the styrene oxide that did not react remained as a racemic mixture. Additionally, it was observed that enantiomerically-enriched styrene oxide did not racemize under the applied reaction conditions. The synthesis of peptidic titanium-phosphonate homochiral catalyst CAT30⁷¹ was described in the previous part of this review.

3. Conclusions

Catalysts containing the phosphonate moiety and their applications have been described in a large number of reports, providing insight into their activity depending on metal elements used, the nature of the organophosphorus components, and an organic or inorganic scaffold. The phosphonate-containing catalysts presented in this review are frequently efficient in more than one described category. From the organic chemist's point of view, this exciting branch of chemistry is worth the interest and development reflected in this review. Considering the development of organic chemistry and reactions such as coupling, epoxidation, reduction or oxidation reactions, etc., modern methods of organic synthesis with catalysts appear to be the most useful. The wide and significant achievements in this field have led to important advances that allow the preparation of more complex organic molecules, useful not only in bioorganic and medicinal chemistry, but in energy-storage materials as well. The application of these efficient and selective methods would help to solve important practical problems in industrial synthesis, safety and environmental protection.

Acknowledgements

The work was supported by grant no. POWR.03.02.00-00-I020/17 co-financed by the European Union through the European Social Fund under the Operational Program Knowledge Education Development.

References

1. Emsley, J.; Hall, D. *The Chemistry of Phosphorus: Environmental, Organic, Inorganic, Biochemical and Spectroscopic Aspects*, Wiley: New York, 1976
2. Goura, J.; Chandrasekhar, V. *Chem. Rev.* **2015**, *115*(14), 6854-6965.
<https://doi.org/10.1021/acs.chemrev.5b00107>
3. Alberti, G.; Costantino, U.; Allulli, S.; Tomassini, N. *J. Inorg. Nucl.* **1978**, *40*(6), 1113-1117.
[https://doi.org/10.1016/0022-1902\(78\)80520-X](https://doi.org/10.1016/0022-1902(78)80520-X)
4. Clearfield, A. *Curr. Opin. Solid State Mater. Sci.* **1996**, *1*, 267-278.
[https://doi.org/10.1016/S1359-0286\(96\)80094-5](https://doi.org/10.1016/S1359-0286(96)80094-5)
5. Zhu, Y. P.; Ren, T. Z.; Yuan, Z. Y. *Catal. Sci. Technol.* **2015**, *5*(9), 4258-4279.
<https://doi.org/10.1039/C5CY00107B>
6. Clearfield, A. *Curr. Opin. Solid State Mater. Sci.* **2002**, *6*, 495-506.
[https://doi.org/10.1016/S1359-0286\(02\)00151-1](https://doi.org/10.1016/S1359-0286(02)00151-1)
7. Mysore Ramesha, B.; Meynen, V. *Mater.* **2020**, *13*(23), 5366-5395.
<https://doi.org/10.3390/ma13235366>
8. Shearan, S. J.; Stock, N.; Emmerling, F.; Demel, J.; Wright, P. A.; Demadis, K. D.; Ruiz Salcedo, I. *Cryst.* **2019**, *9*(5), 270-306.
<https://doi.org/10.3390/cryst9050270>
9. Bhanja, P.; Na, J.; Jing, T.; Lin, J.; Wakihara, T.; Bhaumik, A.; Yamauchi, Y. *Chem. Mater.* **2019**, *31*, 15, 5343-5362.
<https://doi.org/10.1021/acs.chemmater.9b01742>
10. Bhanja, P.; Bhaumik, A. *ChemCatChem.* **2016**, *8*(9), 1607-1616.

<https://doi.org/10.1002/cctc.201501303>

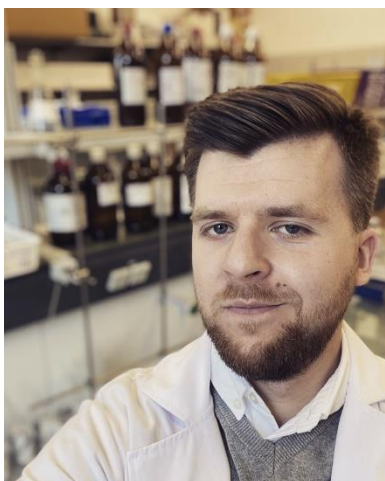
11. Lv, X. W.; Weng, C. C.; Zhu, Y. P.; Yuan, Z. Y. *Small*. **2021**, 17(22), 2005304-20053027.
<https://doi.org/10.1002/sml.202005304>
12. Bao, S.S.; Shimizu, G.K.H.; Zheng, L.M. *Coord. Chem. Rev.* **2019**, 378, 577-594.
<https://doi.org/10.1016/j.ccr.2017.11.029>
13. Shimizu, G. K. H.; Taylor, J. M.; Dawson, K. W. In *Metal Phosphonate Chemistry: From Synthesis to Applications*; Clearfield, A., Demadis, K., Eds.; RSC Publishing: Cambridge, UK, 2012; pp493–524.
14. Levenson, D. A.; Zhang, J.; Szell, P. M.; Bryce, D. L.; Gelfand, B. S.; Huynh, R. P.; Fylstra, N. D.; Shimizu G. K. *Chem. Mater.* **2020**, 32, 679-687.
<https://doi.org/10.1021/acs.chemmater.9b03453>
15. El-Refaei, S. M.; Russo, P. A.; Amsalem, P.; Koch, N.; Pinna, N. *ACS Appl. Nano Mater.* **2020**, 3, 4147-4156.
<https://doi.org/10.1021/acsanm.0c00319>
16. Parangi, T. F.; Chudasama U. V. *ACS Omega* **2019**, 4, 3716-3725.
<https://doi.org/10.1021/acsomega.8b03468>
17. Ma, T.; Zhang, X.; Yuan, Z. *J. Mater. Sci.* **2009**, 44, 6775-6785.
<https://doi.org/10.1007/s10853-009-3576-7>
18. Ma, T. Lin, X.; Yuan, Z. *J. Mater. Chem.* **2010**, 20, 7406-7415.
<https://doi.org/10.1039/C0JM01442G>
19. Shi, X.; Li, J.; Tang, Y.; Yang, Q. *J. Mater. Chem.* **2010**, 20, 6495-6504.
<https://doi.org/10.1039/C0JM00587H>
20. Zheng, L.-M.; Duan, Y. In *Metal Phosphonate Chemistry: From Synthesis to Applications*; Clearfield, A., Demadis, K., Eds.; RSC Publishing: Cambridge, UK, 2012; pp.235-278.
21. Lopez-Diaz, V.; Pellizzeri, T. M. S.; Lijewski, M. D.; Ruhlandt, K.; Zubieta, J. *Inorg. Chim. Acta* **2016**, 441, 109-116.
<https://doi.org/10.1016/j.ica.2015.11.010>
22. Wang, J.; Zhang, R.; Liu, Y.; Wang, Z.; Wang, P.; Zheng, Z. Qin, X.; Zhang, X.; Dai, Y.; Huang, B. *ChemCommun.* **2018**, 54, 7195-7198.
<https://doi.org/10.1039/C8CC02822B>
23. Saha, J.; Chowdhury, D. R.; Jash, P.; Paul, A. *Eur. J. Chem.* **2017**, 23, 12519-12526.
<https://doi.org/10.1002/chem.201700882>
24. Wang, R.; Dong, X.; Du, J.; Zhao, J.; Zang S. *Adv. Mater.* **2018**, 30, 1703711-721.
<https://doi.org/10.1002/adma.201703711>
25. Curini, M.; Rosati, O.; Costantino, U. *Curr. Org. Chem.* **2004**, 8, 591-606.
<https://doi.org/10.2174/1385272043370735>
26. Kirumakki, S.; Samarajeewa, S.; Harwell, R.; Mukherjee, A.; Herberb R. H.; Clearfield A. *Chem. Commun.*, **2008**, 5556-5558.
<https://doi.org/10.1039/B807938B>
27. Kouzu, M.; Yamanaka, S.; Hidaka J.; Tsunomori, M. *Appl. Catal. A*, **2009**, 355, 94-99
<https://doi.org/10.1016/j.apcata.2008.12.003>
28. Pramanik, M.; Bhaumik, A. *J. Mat. Chem. A*. **2013**, 1(37), 11210-11221.
<https://doi.org/10.1039/C3TA12476B>
29. Boronat, M.; Corma, A.; Renz, M.; Sastre, G.; Viruela, P. M. *Eur. J. Chem.*, **2005**,11(23), 6905-6915.
<https://doi.org/10.1002/chem.200500184>

30. Vasylyev, M., Neumann, R. *Chem. Mater.*, **2006**, *18*(12), 2781-2783.
<https://doi.org/10.1021/cm0603506>
31. Gong, B.; Fu, X.; Chen, J.; Li, Y.; Zou, X.; Tu, X.; Ma, L. *J. Catal.*, **2009**, *262*(1), 9-17.
<https://doi.org/10.1016/j.jcat.2008.11.027>
32. Hu, A., Ngo, H. L., Lin, W. *Angew. Chem. Int. Ed.*, **2003**, *42*(48), 6000-6003.
<https://doi.org/10.1002/anie.200351264>
33. Costantino, U., Fringuelli, F., Nocchetti, M., Piermatti, O. *Appl. Catal. A-Gen.*, **2007**, *326*(1), 100-105.
<https://doi.org/10.1016/j.apcata.2007.04.007>
34. Costantino, F.; Vivani, R.; Bastianini, M.; Ortolani, L.; Piermatti, O.; Nocchetti, M.; Vaccaro, L. *ChemComm.* **2015**, *51*(88), 15990-15993.
<https://doi.org/10.1039/C5CC06292F>
35. Varun, B. V.; Dhineshkumar, J.; Bettadapur, K. R.; Siddaraju, Y.; Alagiri, K.; Prabhu, K. R. *Tetrahedron Lett.* **2017**, *58*(9), 803-824.
<https://doi.org/10.1016/j.tetlet.2017.01.035>
36. Devendar, P.; Qu, R. Y.; Kang, W. M.; He, B.; Yang, G. F. *Agric. Food Chem.* **2018**, *66*, 34, 8914-8934.
<https://doi.org/10.1021/acs.jafc.8b03792>
37. Faustini, M.; Nicole, L.; Ruiz-Hitzky, E.; Sanchez, C. *Adv. Funct. Mater.* **2018**, *28*(27), 1704158-88.
<https://doi.org/10.1002/adfm.201704158>
38. Bhattacharyya, B.; Biswas, J. P.; Mishra, S.; Gogoi, N. *Appl. Organomet. Chem.* **2019**, *33*(8), e5017-5030.
<https://doi.org/10.1002/aoc.5017>
39. Borah, S.; Mishra, S.; Cardenas, L.; Gogoi, N. *Eur. J. Inorg. Chem.* **2018**, *2018*(6), 751-758.
<https://doi.org/10.1002/ejic.201701313>
40. Kozell, V.; Giannoni, T.; Nocchetti, M.; Vivani, R.; Piermatti, O.; Vaccaro, L. *Catalysts.* **2017**, *7*(6), 186-206.
<https://doi.org/10.3390/catal7060186>
41. Zhu, Y.-P., Ren, T.-Z., Yuan, Z.-Y. *Catal. Sci. Technol.* **2015**, *5*(9), 4258-4279.
<https://doi.org/10.1039/C5CY00107B>
42. Bhattacharyya, B.; Kalita, A. J.; Guha, A. K.; Gogoi, N. *J. Organomet. Chem.* **2021**, *953*, 122067-75.
<https://doi.org/10.1016/j.jorganchem.2021.122067>
43. Mitrofanov, A.; Brandès, S.; Herbst, F.; Rigolet, S.; Bessmertnykh-Lemeune, A.; Beletskaya, I. *J. Mat. Chem. A*, **2017**, *5*(24), 12216-12235.
<https://doi.org/10.1039/C7TA01195D>
44. Hu, H.; Xin, J. H.; Hu, H.; Wang, X.; Miao, D.; Liu, Y. *J. Mater. Chem. A*. **2015**, *3*(21), 11157-11182.
<https://doi.org/10.1039/C5TA00753D>
45. Hey, D. A.; Reich, R. M.; Baratta, W.; Kühn, F. E. *Coord. Chem. Rev.* **2018**, *374*, 114-132.
<https://doi.org/10.1016/j.ccr.2018.06.005>
46. Costantino, F.; Nocchetti, M.; Bastianini, M.; Lavacchi, A.; Caporali, M.; Liguori, F. *ACS Appl. Nano Mater.* **2018**, *1*(4), 1750-1757.
<https://doi.org/10.1021/acsanm.8b00193>
47. Forato, F.; Belhboub, A.; Monot, J.; Petit, M.; Benoit, R.; Sarou-Kanian, V.; Fayon, F.; Jacquemin, D.; Queffelec, C.; Bujoli, B. *Eur. J. Chem.*, **2018**, *24*(10), 2457-2465.
<https://doi.org/10.1002/chem.201705283>
48. Smith, M B.; March, J. *March's Advanced Organic Chemistry*, 5th Ed. Wiley&Sons, New York, 2001.
49. Zhang, D.; Dumont, M.-J. *J. Polym. Sci. A Polym. Chem.* **2017**, *55*(9), 1478-1492.
<https://doi.org/10.1002/pola.28527>

50. Hu, L.; Li, N.; Dai, X.; Guo, Y.; Jiang, Y.; He, A.; Xu, J. *J. Energy Chem.* **2019**, *37*, 82-92.
<https://doi.org/10.1016/j.jechem.2018.12.001>
51. Wang, J.; Wang, R.; Zi, H.; Wang, H.; Xia, Y.; Liu, X. *J. Chin. Chem. Soc.* **2018**, *65*(6), 750-759.
<https://doi.org/10.1002/jccs.201700309>
52. Du, Y.; Feng, D.; Wan, J.; Ma, X. *Appl. Catal. A: Gen.* **2014**, *479*, 49-58.
<https://doi.org/10.1016/j.apcata.2014.03.039>
53. Chen, T.; Ma, X.; Wang, X.; Wang, Q.; Zhou, J.; Tang, Q. *Dalton Trans.* **2011**, *40*(13), 3325-3335.
<https://doi.org/10.1039/C0DT00786B>
54. Xu, X.; Wang, R.; Wan, J.; Ma, X.; Peng, J. *RSC Advances*, **2013**, *3*(19), 6747-6751.
<https://doi.org/10.1039/C3RA22057E>
55. Ferlin, F.; Cappelletti, M.; Vivani, R.; Pica, M.; Piermatti, O.; Vaccaro, L. *Green Chem.* **2019**, *21*(3), 614-626.
<https://doi.org/10.1039/C8GC03513J>
56. Pica, M.; Donnadio, A.; Capitani, D.; Vivani, R.; Troni, E.; Casciola, M. *Inorg. Chem.* **2011**, *50*(22), 11623-11630.
<https://doi.org/10.1021/ic2015594>
57. Zhou, A.; Li, J.; Wang, G.; Xu, Q. *Appl. Surf. Sci.* **2020**, *506*, 144570.
<https://doi.org/10.1016/j.apsusc.2019.144570>
58. Zhu, Y.-P., Liu, Y.-L., Ren, T.-Z., Yuan, Z.-Y. *RSC Adv.*, **2014**, *4*(31), 16018-16021.
<https://doi.org/10.1039/C4RA01466A>
59. Armakola, E.; Colodrero, R. M. P.; Bazaga-García, M.; Salcedo, I. R.; Choquesillo-Lazarte, D.; Cabeza, A.; Demadis, K. D. *Inorg. Chem.* **2018**, *57*, 10656-10666.
<https://doi.org/10.1021/acs.inorgchem.8b01315>
60. Bhanja, P.; Ghosh, K.; Islam, S. S.; Patra, A. K.; Islam, S. M.; Bhaumik, A. *ACS Sustain. Chem. Eng.*, **2016**, *4*(12), 7147-7157.
<http://doi:10.1021/acssuschemeng.6b02023>
61. Mo, S.; Zhao, X.; Chen, Y.; Liu, L.; Wang, R.; Xu, Q. *Mater. Chem. Phys.* **2013**, *140*(1), 228-235.
<https://doi.org/10.1016/j.matchemphys.2013.03.026>
62. Thornburg, N. E.; Notestein, J. M. *ChemCatChem*, **2017**, *9*(19), 3714-3724.
<https://doi.org/10.1002/cctc.201700526>
63. Rocha, G. M.; Santos, T. M.; Bispo, C. S. *Catal. Lett.* **2011**, *141*(1), 100-110.
<https://doi.org/10.1007/s10562-010-0481-2>
64. Dutta, A.; Pramanik, M.; Patra, A. K.; Nandi, M.; Uyama, H.; Bhaumik, A. *ChemComm.* **2012**, *48*(53), 6738-6740.
<https://doi.org/10.1039/C2CC32298F>
65. Huang, J.; Yuan, L.; Cai, J.; Liu, Z. *Microporous Mesoporous Mater.* **2015**, *214*, 121-126.
<https://doi.org/10.1016/j.micromeso.2015.05.003>
66. He, S.; Liu, X.; Zhao, H.; Zhu, Y.; Zhang, F. *J. Colloid Interface Sci.* **2015**, *437*, 58-64.
<https://doi.org/10.1016/j.jcis.2014.08.065>
67. Tu, X.; Fu, X.; Hu, X.; Li, Y. *Inorg. Chem. Commun.* **2010**, *13*(3), 404-407.
<https://doi.org/10.1016/j.inoche.2009.12.034>
68. Shen, H.; Fu, X.; Bao, H.; Chen, J.; Gong, B. *Polym. Adv. Technol.* **2009**, *20*(2), 77-83.
<https://doi.org/10.1002/pat.1214>
69. Huang, J.; Cai, J.; Li, C. M.; Fu, X. K. *Inorg. Chem. Commun.*, **2014**, *48*, 36-39.
<https://doi:10.1016/j.inoche.2014.08.006>

70. Milo, A.; Neumann, R. *ChemComm.*, **2011**, 47(9), 2535-2537.
<https://doi.org/10.1039/C0CC04205F>
71. Milo, A.; Neumann, R. *Adv. Synt. Catal.*, **2010**, 352(13), 2159-2165.
<https://doi.org/10.1002/adsc.201000373>
72. Zou, X.; Nie, X.; Tan, Z.; Shi, K.; Wang, C.; Wang, Y.; Zhao, X. *Catalysts*. **2019**, 9(9), 710-722.
<https://doi.org/10.3390/catal9090710>
73. Fu, H., You, F., Li, H., & He, L. *Front. Chem.* **2019**, 7:525.
<https://doi.org/10.3389/fchem.2019.00525>
74. Ai, J.; Min, X.; Gao, C.-Y.; Tian, H.-R.; Dang, S.; Sun, Z.-M. *Dalton Trans.*, **2017**, 46(20), 6756-6761.
<https://doi.org/10.1039/C7DT00739F>
75. Gao, C.-Y.; Yang, Y.; Xu, N.; Liu, J.; Duan, L.; Chen, X.; Bao, M. *Cryst Growth Des.*, **2021**, 21(3), 1413-1417.
<https://doi.org/10.1021/acs.cgd.0c01628>
76. Yang, Y.; Gao, C.-Y.; Tian, H.-R.; Ai, J.; Min, X.; Sun, Z.-M. *ChemComm.*, **2018**, 54(14), 1758-1761.
<https://doi.org/10.1039/C7CC09867G>
77. Ghosh, S.; Bhanja, P.; Salam, N.; Khatun, R.; Bhaumik, A., Islam, S. M. *Catal.* **2018**, 309, 253-262.
<https://doi.org/10.1016/j.cattod.2017.05.093>
78. Rosati, O.; Lanari, D.; Scavo, R.; Persia, D.; Marmottini, F.; Nocchetti, M.; Curini, M.; Piermatti, O. *Micropor. Mesopor. Mat.* **2018**, 268, 251-259.
<https://doi.org/10.1016/j.micromeso.2018.04.035>
79. Calogero, S.; Lanari, D.; Orrù, M.; Piermatti, O.; Pizzo, F.; Vaccaro, L. *J. Catal.* **2011**, 282(1), 112-119.
<https://doi.org/10.1016/j.jcat.2011.06.004>
80. Arpanahi, F.; Mombeni Goodajdar, B. *J. Inorg. Organomet. Polym. Mater.* **2020**, 30(7), 2572-2581.
<https://doi.org/10.1007/s10904-020-01530-9>
81. Dutta, A.; Mondal, J.; Patra, A. K.; Bhaumik, A. *Eur. J. Chem.* **2012**, 18(42), 13372-13378.
<https://doi.org/10.1002/chem.201201350>
82. Liu, X.; Min, X.; Liu, H.; Cao, Y.; Liu, Y.; Han, M.; Sun, Z.-M.; Ji, S. *Sustain. Energy Fuels*. **2020**, 4(11), 5795-5801.
<https://doi.org/10.1039/D0SE01006E>
83. de Mello, D.; Kumar, M.; Tabassum, G.; Jain, T.; Chen, S. K.; Caratzoulas, S., Li, X.; Vlachos D.G.; Han, S.-I.; Scott S. L.; Dauenhauer P.; Tsapatsis, M.. *Angew. Chem. Int. Ed.*, **2020**, 59(32), 13260-13266.
<https://doi.org/10.1002/anie.202001332>

Authors' Biographies



Mateusz Klarek was born in 1994 in Poznań, Poland. In 2016, he earned Bachelor's degree in general chemistry (B.Sc.) from Adam Mickiewicz University (AMU). In 2018, he defended his Master's dissertation (M.Sc.) – Repetitive batch borylative coupling of olefins with vinylboranes in green solvents, written under the supervision of Professor Piotr Pawluć. Currently, he is a PhD candidate of The Department of Synthesis and Structure of Organic Compounds at Adam Mickiewicz University (supervisor: Prof. Magdalena Rapp). His research area covers synthesis and structural studies of fluorine and phosphorus containing organic molecules, especially aziridines and aminophosphonates as biologically active compounds.



Magdalena Rapp graduated in chemistry in 1999 at Adam Mickiewicz University (AMU) in Poznań. In 2003, she defended her doctorate on the synthesis and photochemistry of pyrimidines under the supervision of Prof. Golankiewicz at the same faculty. In the period 2004-2006 she completed a postdoctoral fellowship in the group of Prof. Stanisław Wnuk at the FIU University in Miami, USA, where she gained experience in the chemistry of sugars and nucleosides. In 2006, she started working as an assistant professor at the Department of Synthesis and Structure of Organic Compounds at the Faculty of Chemistry Adam Mickiewicz University in the research group of Prof. Henryk Koroniak. In 2019, she obtained her habilitation for the work related to the synthesis and

stereochemistry of natural compounds analogues. Her research interests focus on both classical and modern organic synthesis, in particular the phosphorus and fluorine organic chemistry.

This paper is an open access article distributed under the terms of the Creative Commons Attribution (CC BY) license (<http://creativecommons.org/licenses/by/4.0/>)